T.C.
ISTANBUL UNIVERSITY-CERRAHPASA
INSTITUTE OF GRADUATE STUDIES

M.Sc. THESIS

PRODUCTION OF METAMATERIALS AND SMART MATERIALS BY RAPID PROTOTYPING METHOD

MOHAMAD ATTAR

SUPERVISOR
Assoc. Prof. Dr. İlven MUTLU

Department of Nanoscience and Nanoengineering

Nanoscience and Nanoengineering Programme

ISTANBUL- August, 2020

This study was accepted on 27/8/2020 as a M. Sc. thesis in ....., ... by the following Committee.

Examining Committee Members

Assoc. Prof. Dr. İlven MUTLU(Supervisor)
İstanbul University-Cerrahpaşa
Faculty of Engineering

Assist. Prof. Dr. Ümran KURTAN
Istanbul University-Cerrahpasa
Vocational School of Technical Sciences

Assoc. Prof. Dr. Derya DIŞPINAR
Istanbul Technical University
Faculty of Chemical and Metallurgical Engineering

Academic Title Name SURNAME
University
Faculty

Academic Title Name SURNAME
University
Faculty

As required by the 9/2 and 22/2 articles of the Graduate Education Regulation which was published in the Official Gazette on 20.04.2016, this graduate thesis is reported as in accordance with criteria determined by the Institute of Graduate Sttudies by using the plagiarism software to which Istanbul University-Cerrahpasa is a subscriber.

This thesis is supported by the project numbered 34045 of Istanbul University-Cerrahpaşa Scientific Research Projects Executive Secreteriat.

FOREWORD

I would like to thank my family members who have always supported me in this proces

August 2020 Mohamad ATTAR

TABLE OF CONTENTS

Page

FOREWORD ..... **iv**
TABLE OF CONTENTS ..... **v**
LIST OF FIGURES ..... **vii**
LIST OF TABLES ..... **ix**
LIST OF SYMBOLS AND ABBREVIATIONS ..... **x**
ÖZET ..... **xi**
SUMMARY ..... **xii**
1. INTRODUCTION **1**
1.1. SMART MATERIALS……1
1.2. METAMATERIALS……..2
1.3. SHAPE MEMORY MATERIALS…….8.
1.4. SELF HEALING MATERIALS……16
1.5. CORONARY STENTS……..18
1.6. RAPID PROTOTYPING……..…20
1.7. POWDER METALLURGY…….…24
1.8. LITERATURE REVIEW…….…….26
2. MATERIALS AND METHODS **28**
2.1. PRODUCTION OF POLYMER MATERIALS……..28
2.2. PRODUCTION OF METAL ALLOYS……..…….31
2.3. SHAPE MEMORY TRAINING……..33
2.4. CHARACTERIZATION……..34
2.4.1. Microstructure…….……34
2.4.2. Mechanical Properties…….……35
3. RESULTS **36**
3.1. POLYMER MATERIALS……36
3.1.1. Microstructure…….…36
3.1.2. Mechanical Properties…….……38
3.2. METAL ALLOYS……42
3.2.1. Microstructure……..42
3.2.2. Mechanical Properties……..48

4. DISCUSSION 52
5. CONCLUSION AND RECOMMENDATIONS 54
REFERENCES 56
CURRICULUM VITAE 58

LIST OF FIGURES

Page

Figure 1.1 Classification of the mechanical metamaterials ……..…….**3.**

Figure 1.2 Non-auxetic and auxetic mateials under tensile and compression loads ……**4.**

Figure 1.3 Re-entrant auxetic and meta-chiral structures ……**4.**

Figure 1.4 Star shaped systems and rotating rhombi/parallelogram systems …….……**5.**

Figure 1.5 Indentation properties of traditional and auxetic materials ……..……**6.**

Figure 1.6 Auxetic filter application ……..……**6.**

Figure 1.7 Auxetix stent application ……..……**7.**

Figure 1.8 Phases and crystal structures in the shape memory alloys ……**9.**

Figure 1.9 Stress-temperature diagram of shape memory alloys …….……**10.**

Figure 1.10 One-way shape memory effect …….……**10.**

Figure 1.11 Superelastic properties ……..……**11.**

Figure 1.12 Shape memory mechanism in polymers …….……..……**14.**

Figure 1.13 Shape memory polymers …….……..….**15.**

Figure 1.14 Self-healing of the polymers ……**17.**

Figure 1.15 Placement of a stent …….……**18.**

Figure 1.16 Production steps of a stent ……**19.**

Figure 1.17 Photo-polymerization method ……..……**21.**

Figure 1.18 Fused deposition modelling (FDM) method …….……**21.**

Figure 1.19 Selective laser sintering (SLS) method ……..……**22.**

Figure 1.20 Electron beam melting (EBM) method …….……**22.**

Figure 1.21 Classification of the additive manufacturing method ……..…..……**23.**

Figure 1.22 Main steps of the powder metallurgy method ……..…..……**25.**

Figure 2.1 Stereolithography based rapid prototyping method ……..…..……**28.**

Figure 2.2 Replica method **……..……..…….29.**

Figure 2.3 Polyurethane a) polymerisation mechanism and b) solid specimens **……..…….30.**

Figure 2.4 a) Ball mill and hydraulic press, b) sintering furnace **……..…….31.**

Figure 2.5 Powder injection molding method **…….32.**

Figure 2.6 Shape memory training heat treatment **……..……..….33.**

Figure 2.7 Tension-compression test device **…….….35.**

Figure 3.1 Pictures of a) metamaterial prototype, b) negative mould, c) filled metamaterial **.36.**

Figure 3.2 SEM pictures of microstructure of a) PU specimen, b) silicone specimen **…….37.**

Figure 3.3 Photographs during compression tests of PU a) lateral, b) vertical **…….…..38.**

Figure 3.4 Photographs during compression tests of PU composites a) lateral, b) vertical **….39.**

Figure 3.5 a) Stress-strain curves of the metamaterial PU, b) deformation mechanism ..**….40.**

Figure 3.6 Shape memory effect in the PU specimens …….**….41.**

Figure 3.7 SEM picture of a) Ni, b) Ti, c) Co, d) Sn powders ……**….42.**

Figure 3.8 a) SEM picture of microstructure, b) photograph of sintered Ti-Ni alloy ……..**….43.**

Figure 3.9 XRD results of the alloys a) Ti, b) Ni, c) Ti-Ni, d) Ti-Ni-Co-Sn alloys …….**….44.**

Figure 3.10 a) DSC of Ti-Ni-Co-Sn, b) DSC of Ti-Ni, c) DTA of Ti-Ni **……..45.**

Figure 3.11 Corrosion test results of the alloys…… ……..**46.**

Figure 3.12 Effect of a) Co and b) Sn on polarization resistance and corrosion rate …….**….47.**

Figure 3.13 Effect of sintering temperature on a) Young's modulus, and b) yield strength **….48.**

Figure 3.14 Effect of aging temperature on a) Young's modulus, and b) yield strength l .**….49.**

Figure 3.15 Effect of Co and Sn on (a) Young's modulus, and (b) yield strength al ….**…….50.**

Figure 3.16 Effect of temperature on the Young's modulus (microstructure) of the alll ..**….51.**

LIST OF TABLES

Page

Table 1.1 Shape memory materials ……...……**12.**

Table 1.2 Properties of the NiTi ……..……**13.**

Table 2.1 Compositions of the Ti-Ni based alloys ……**31.**

LIST OF SYMBOLS AND ABBREVIATIONS

Symbol	Explanation
T	**:** Temperature
t	**:** Time
º	**:** Degree
α	**:** Alpha
β	**:** Beta

Abbreviation	Explanation
g	**:** Gram
mg	**:** Mili gram
mm	**:** Mili meter
nm	**:** Nano meter
ppm	**:** Parts per million
PVA	**:** Polyvinylalcohol
µm	**:** Micro meter
MA	**:** Mechanical alloying
OCP	**:** Open circuit potential

ÖZET

YÜKSEK LİSANS TEZİ

METAMALZEMELERİN VE AKILLI MALZEMELERİN HIZLI PROTOTİPLEME YÖNTEMİ İLE ÜRETİLMESİ

MOHAMAD ATTAR

İstanbul Üniversitesi-Cerrahpasa

Lisansüstü Eğitim Enstitüsü

Nanobilim ve Nanomühendislik Anabilim Dalı

Danışman : Doç. Dr. İLVEN MUTLU

Bu tez çalışmasında, mekanik meta-malzeme (ökzetik malzeme) ve akıllı malzemelerin (şekil bellekli alaşım) eklemeli üretim esaslı hızlı prototipleme ve replika yöntemi ile üretimi ve incelenmesi gerçekleştirilmiştir. Pozitif kalıplar (prototip) stereolitografi esaslı hızlı prototipleme yöntemi ile üretilmiştir. Hammadde olarak akrilik esaslı fotopolimer reçine kullanılmıştır. Daha sonra aljinat kalıplama (replika) yöntemi ile silikon ürünler (koroner stent, üretal stent, soluk borusu stenti, tampon, tendon grefti, doku grefti) üretilmiştir. Negative kalıp malzemesi olarak aljinat kullanılmıştır. Oda sıcaklığında vulkanize olan silikon reçine aljinat kalıp boşluğuna dökülmüştür. Takviye olarak nano-boyutlu TiO_2 tozu ve karbon fiber ilave edilerek silikon matrisli kompozit malzeme üretimi gerçekleştirilmiştir. Ayrıca ökzetik poliüretan takviyeli silikon matrisli kompozit üretimi de gerçekleştirilmiştir. Akıllı malzeme esaslı şekil bellekli Ni-Ti alaşımı ise toz metalurjisi ve toz enjeksiyon kalıplama ile üretilmiştir. Şekil bellekli Ni-Ti (nitinol) alaşımının stent uygulamaları için geliştirilmesi amaçlanmıştır. Üretilen malzemelerin mikroyapısı ve mekanik özellikleri incelenmiştir. Malzemelerin sertlik, çekme-basma davranışı, elastisite modülü gibi mekanik özellikleri belirlenmiştir.
Ağustos 2020, 70. sayfa.

Anahtar kelimeler: Şekil bellek, akıllı malzeme, hızlı prototipleme, metamalzeme, stent

SUMMARY

M.Sc. THESIS

PRODUCTION OF METAMATERIALS AND SMART MATERIALS BY RAPID PROTOTYPING METHOD

MOHAMAD ATTAR

Istanbul University-Cerrahpasa

Institute of Graduate Studies

Department of Nanoscience and Nanoengineering

Supervisor : Assoc. Prof. Dr. İLVEN MUTLU

In this thesis, production and characterization of mechanical metamaterials (auxetic materials) and smart materials (shape memory alloys) were carried out. Materials were produced by additive manufacturing based rapid prototyping and replica method. Positive moulds (prototypes) were produced by stereolythografi based rapid prototyping method. Acrylic based photopolymer was used as a raw material. Then, silicone products (coronary stents, urethal sents, grafts) was produced by alginate molding (replica method). Alginat was used as a negative mould. Room temperature vulcanised silicone resin was poured into the mould. Several reinforcement materials was used for the production of composite materials. In addition, auxetic polyurethane reinforced silicone matrix composites were manufactured. Shape memory (smart material) Ni-Ti alloys were produced by powder metallurgy and powder injection moulding methods. Microstructure and mechanical properties of the materials were investigated. Hardness, tension-compression behaviour, elastic modulus parameters of the materials were determined.

August 2020, 70. pages.

Keywords: Shape memory, smart material, rapid prototyping, metamaterial, stent

1. INTRODUCTION

1.1. SMART MATERIALS

Smart materials (also known as responsive materials) have several uniquie engineering properties like changing the shape (geometry), resistivity, color. The manufacturing and use of the smart materials (responsive materials) is relatively new topic. In general, the smart materials are manufactured to make a response in a controlled and desired way. Smart materials can be used mainly in the sensor applications, in the actuator applications or in the artificial muscle (robotic) applications. By using of the several types of the smart materials, several important engineering devices can be manufactured.

Smart materials (SM) can be classified as two general types;

- Sensors (optical fibers, piezoelectric polymers)
- Actuators (shape memory materials, piezoelectric ceramics, magnetostrictive materials)

In general, sensors are used in the detection of some canges and produce a response for these events. Actuators are used to control a system. In general, the actuators can make a response to electrical, thermal, or magnetic forces. Actuators usually need a controlling signal tocontrol a system. In general, shape memory materials can remember their initial geometry (shape) under the application of an external forces [1].

Classification of the smart material:

- Property change capacity
- Size-location
- Capacity to change energy
- Reversibility (bi-direction)

There are 2 general types of smart materials: first type alters their some properties, by an external control. Second type transforms energy from one form to another.

1.2. METAMATERIALS

Metamaterials are artificial composite products not observable in the nature. Their unusual engineering behaviours are attributed to for their microstructural arranged geometry, not their chemical composition (material properties). The arrangement of their geometry/shape (macro-architecture) provides very unique and usefull engineering properties. Meta-materials are macroscopic composites with 3-dimensional, cellular architecture designed to produce optimized properties, not available in nature.

Metamaterials;

- Mechanical metamaterials (auxetics) having negative Poisson's ratio (NPR)
- Electronical/magnetical type metamaterials having negative diffraction index

Metamaterials are novel and unique manmade composite materials with unconventional electromagnetic (metamaterials) and mechanical properties (auxetic metamaterials) that are not seen in the natural materials.

Mechanical metamaterial (auxetic) are metamaterials with very special mechanical properties based on their structure (geometry or architecture).

In general, the metamaterials show unusual engineering behaviours such as elastic modulus, density, impact absorption, acoustic and phononic properties, heat conduction, and negative Poisson's ratio (NPR) [1,2].

Figure given below shows the classification of the mechanical metamaterials according to their elastic modulus, shear (bulk) modulus, and Poisson's ratio values [2].

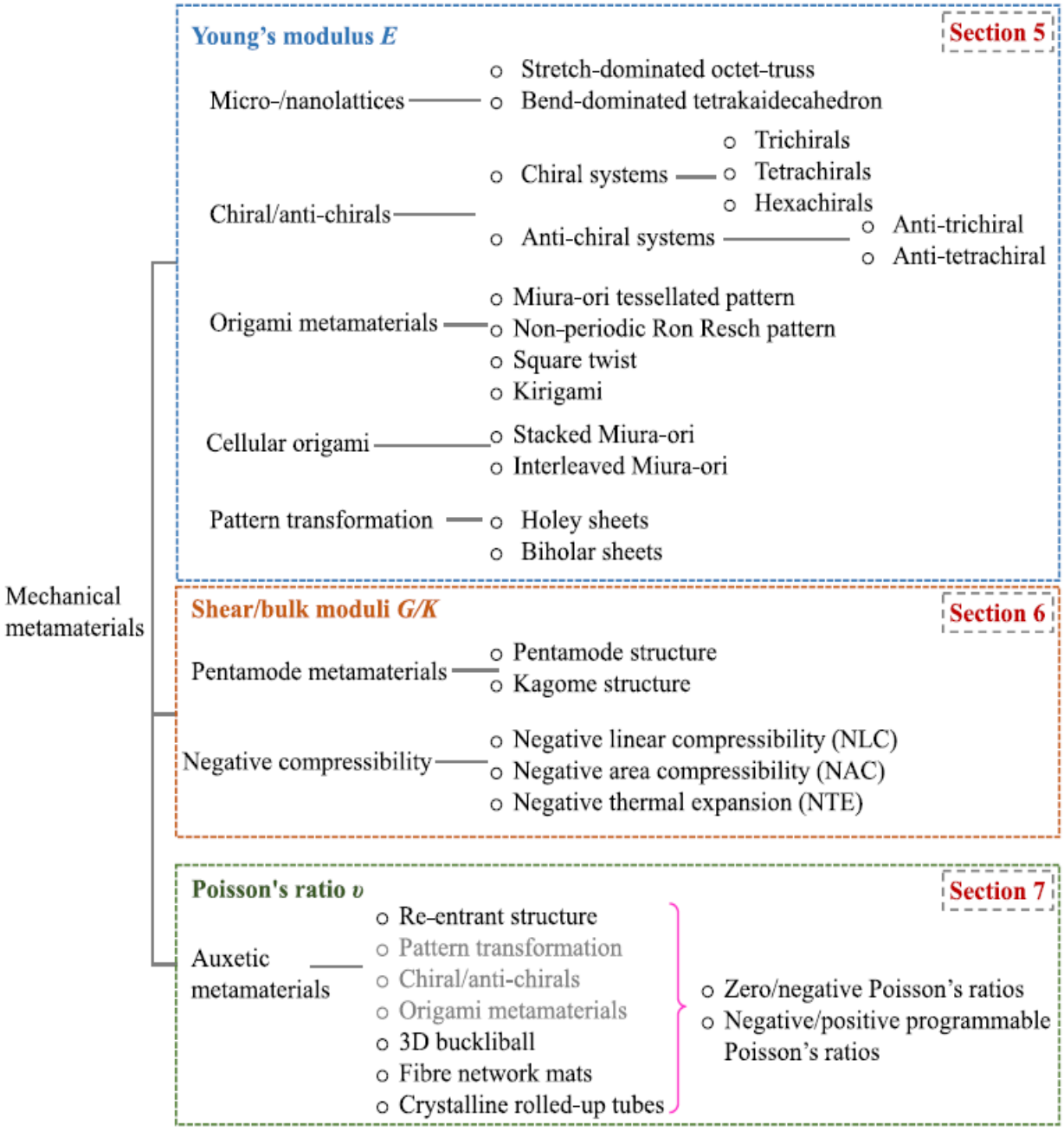

Figure 1.1: Classification of the mechanical metamaterials [2]

Figure shown below illustrates the behaviours of the non-auxetic and auxetic metamaterial under tensile and compression forces (loads) [3].

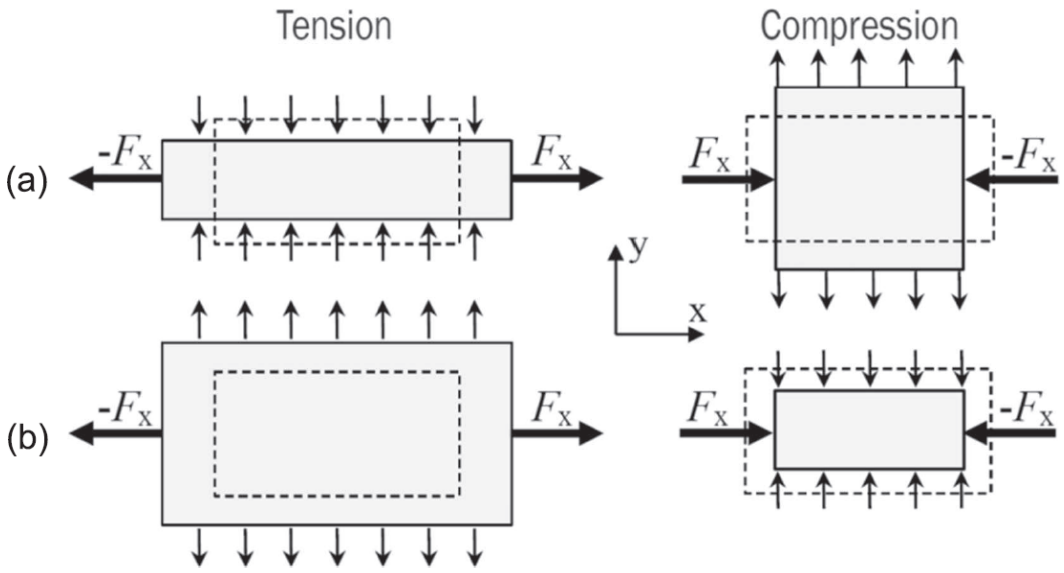

Figure 1.2: Non-auxetic and auxetic mateials under tensile and compression loads [3]

Figure shown below illustrates the re-entrant auxeticand chiral auxetic geometries with different ribs attached at nodes such as 6 ribs; r ribs 3 ribs [3]

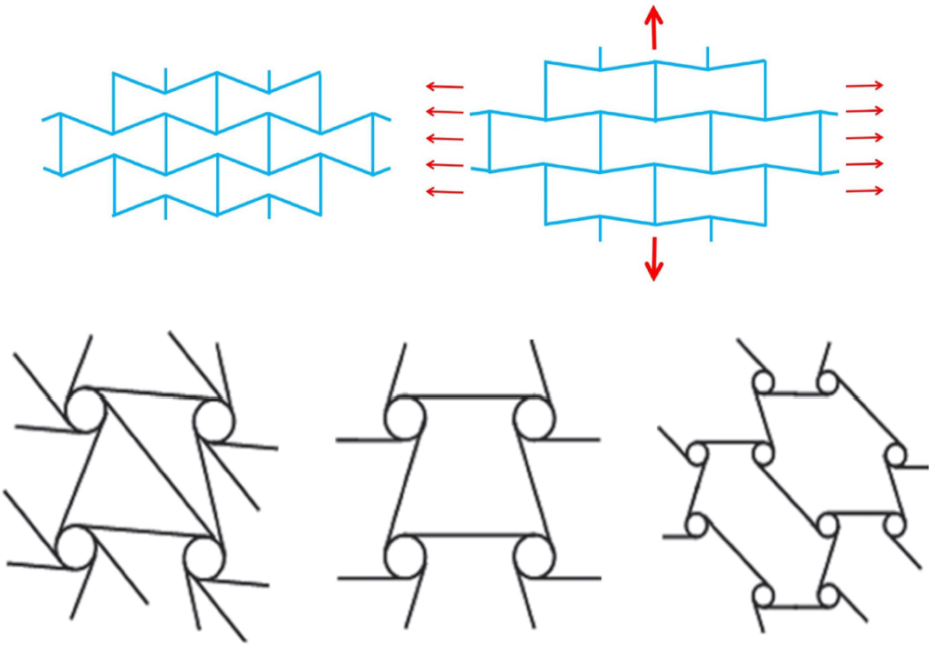

Figure 1.3: Re-entrant auxetic and meta-chiral structures [3]

Figure given below shows the different star-shaped metamaterial geometries, which having different rotational symmetries. In addition, rhombi type and rotating parallelogram type metamaterial shapes can be seen [3]

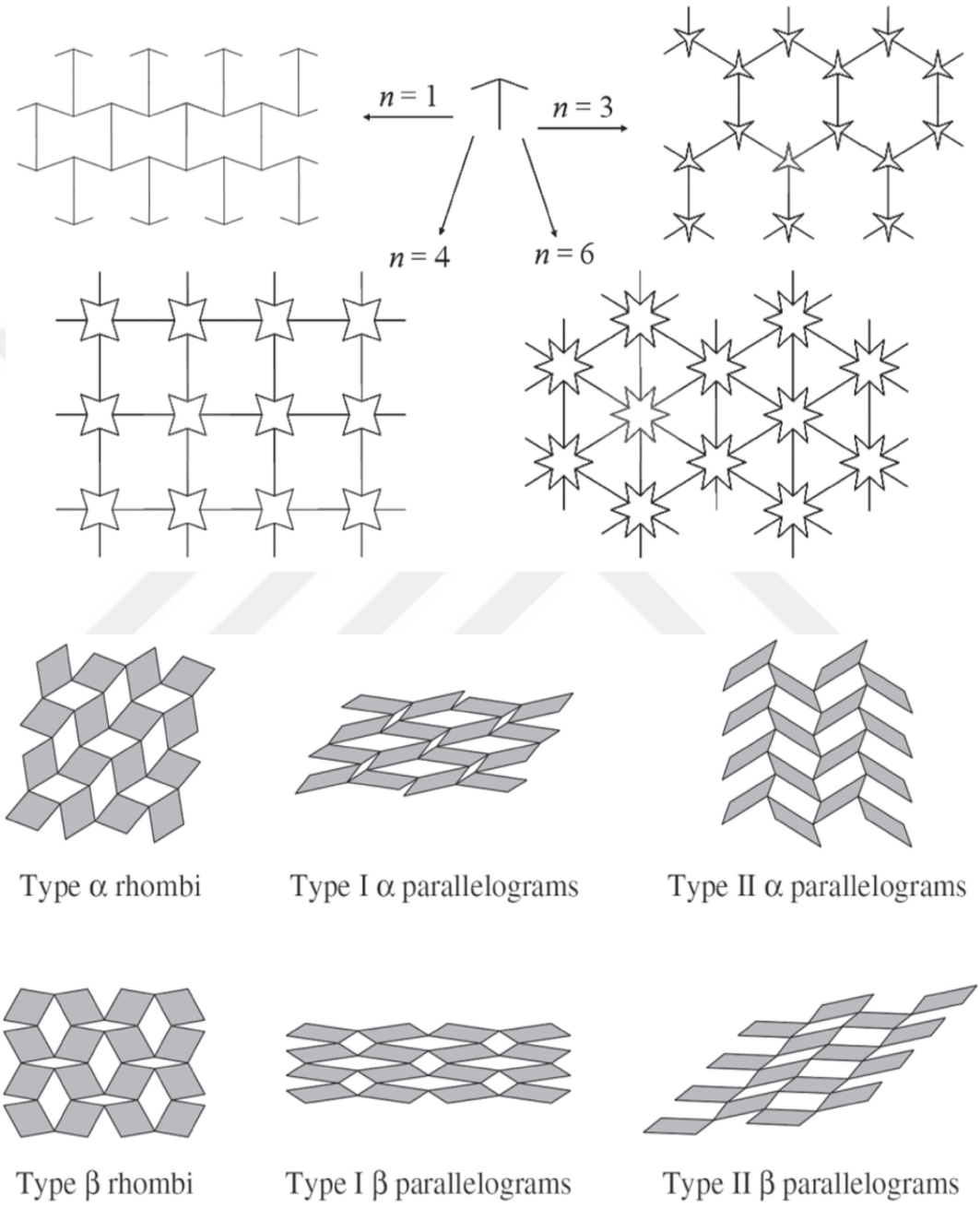

Figure 1.4: Star shaped systems and rotating rhombi/parallelogram systems [3]

Figure shown below illustrates the indentation (hardness) behaviours of a traditional material and a mechanical metamaterial (auxetic) [3]. Auxetic materials show higher hardness, as shown in the figure. In addition, mechanical metamaterials (auxetic) can be employed as a smart filters, which having a variable permeability, as shown in the figure [3]

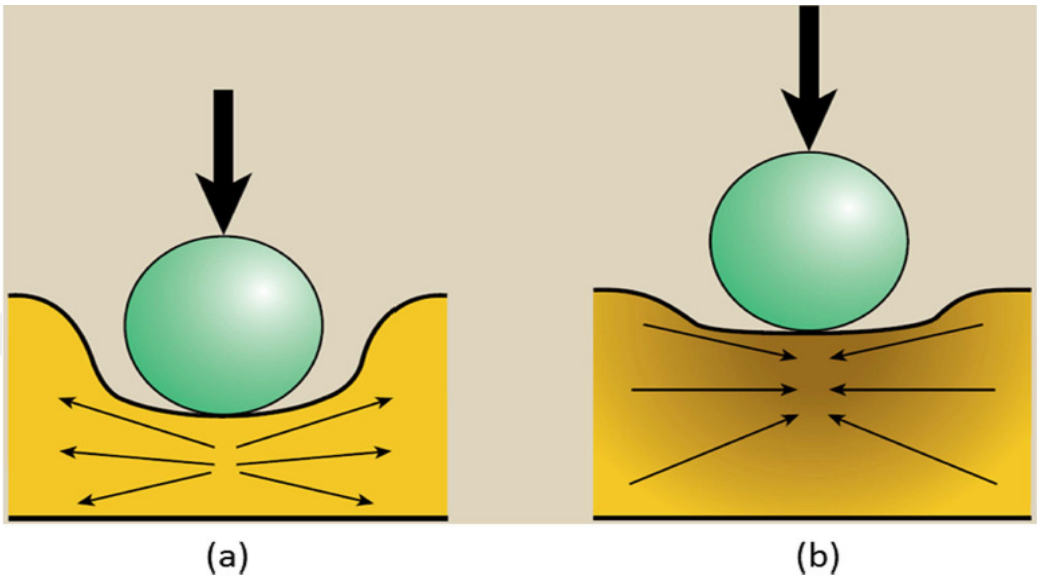

Figure 1.5: Indentation properties of traditional and auxetic materials [3]

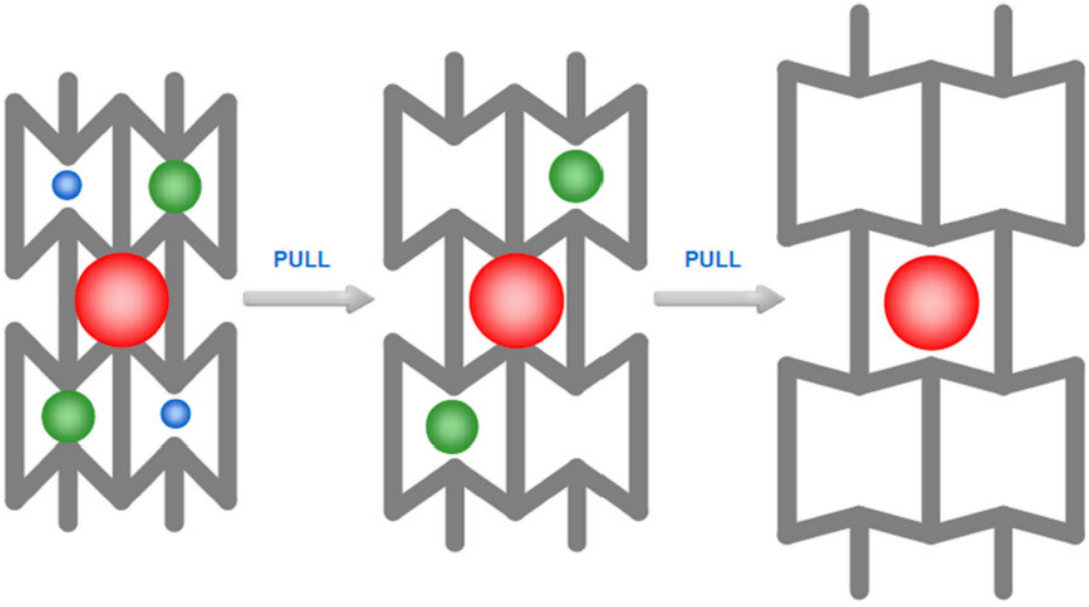

Figure 1.6: Auxetic filter application [3]

Figure given below illustrates the coronary or peripheral stent applications of the mechanical metamaterials (auxetic). In general, the auxetic behaviour provides a radial strength to the coronary or peripheral stents [3].

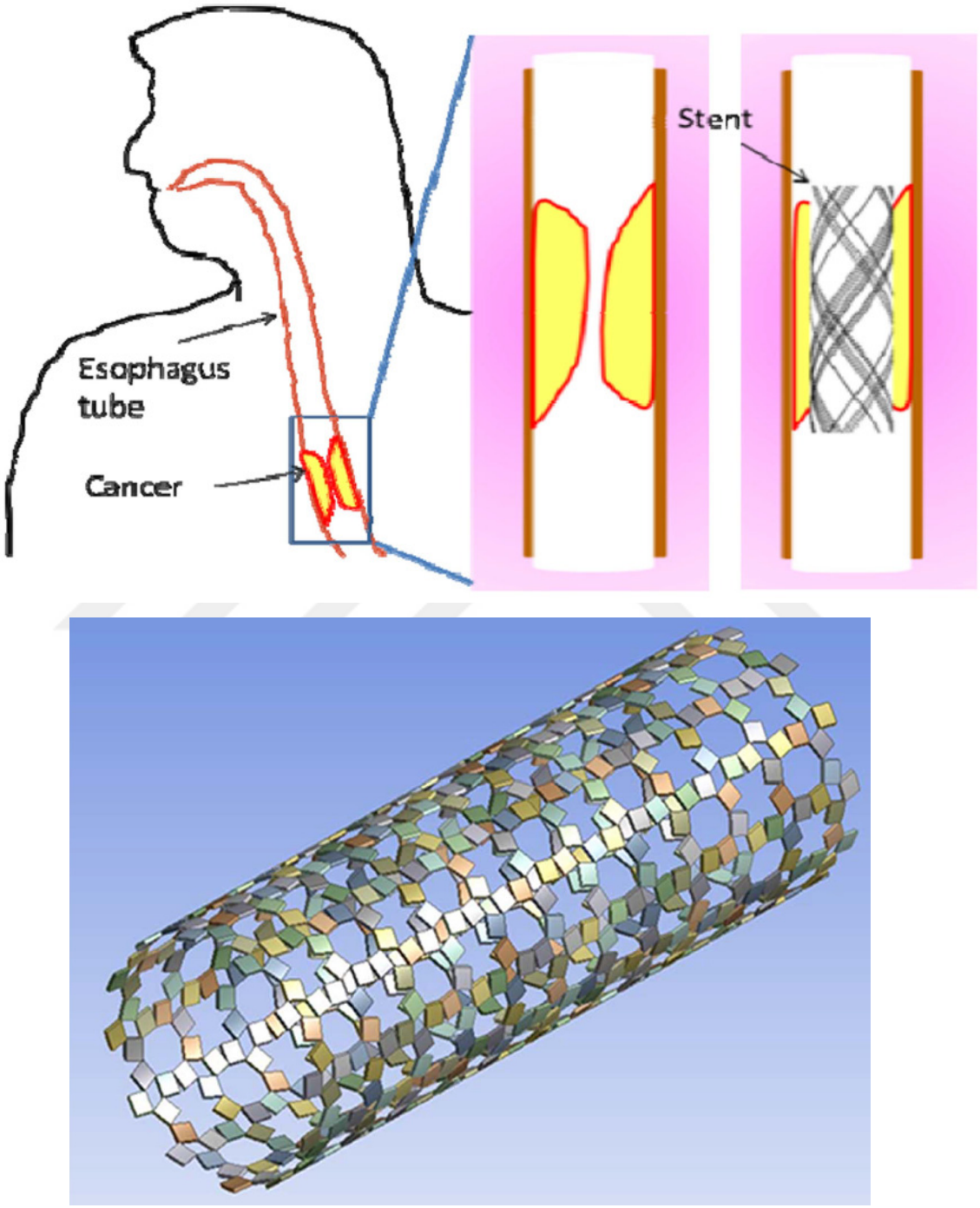

Figure 1.7: Auxetix stent application [3]

1.3. SHAPE MEMORY MATERIALS

A shape memory alloy (SMA) is an alloy that programmed to remember its first shape and after a specific deformation it can returns to this first shape by a specific heat treatment (heating). In general, the shape memory (SM) alloys can return to the undeformed first shape by heating (shape memory effect) or by removal of the stress (superelastic effect). This unique property is due to the solid-solid, diffusionless, reversible and displacive phase change by shear. SM alloys can exist in 3 structures (twinned martensite, detwinned martensite and austenite). In general, shape memory alloys can be employed in the robotics applications, aviation applications and biomedical applications. In addition, shape memory alloys can be employed in the dental implant applications, and in coronary stents.

Shape memory alloys (SMAs), can be shaped (deformed), and then after subsequent deformation, they can remember to their first geometry when this same force is applied. In general, the mechanism of the shape memory effect (SME) can be attributed to the crystallographic reversibility of alloy. Austenite phase can be obtained above the transus temperature, while the martensite phase can be obtained below this temperature. After deformation at the martensite region, and then subsequeint heating, transforms from martensite to the austenite and remember their first geometry.

Shape memory materials can be classified as;

- Temperature-induced shape memory (Traditional)
- Stress-induced shape memory (Superelasticity or Pseudoelasticity)

Martensite transformation (diffusion-less transformation) :

- Thermoelastic transformation
- Non-thermoelastic transformation

Thermoelastic martensitic transformation occur by twinning at the twin-boundaries and return to the first geometry.

Non-thermoelastic martensitic transformation occur by the slip of the dislocations. Non-thermoelastic martensitic transformation can not return to first shape).

In general, there are 2 types of composition invariant transformations.

- ❑ Massive transformation (civilian or diffusional)
- ❑ Martensitic transformation (military or difusion-less)

Massive transformation is short-range diffusional transformation which occur without any orientation. It can be described as a civilian transformation because its atoms can diffuse individually. Martensitic transformation (military transformation) is a change in phase. There is no need to diffusion in the military transformations. There is no long-range diffusion, also there is no change in the chemical composition. In the martensitic transformation (military transformation), there is a shear-like deformation.

General Requirements for the Shape Memory and Superelasticity Behaviours

- Martensitic transformations must be thermoelastic
- There must be an ordering in the microstructure
- Deformation mode must be twinning.
- Twinning-Detwinning must be equal.

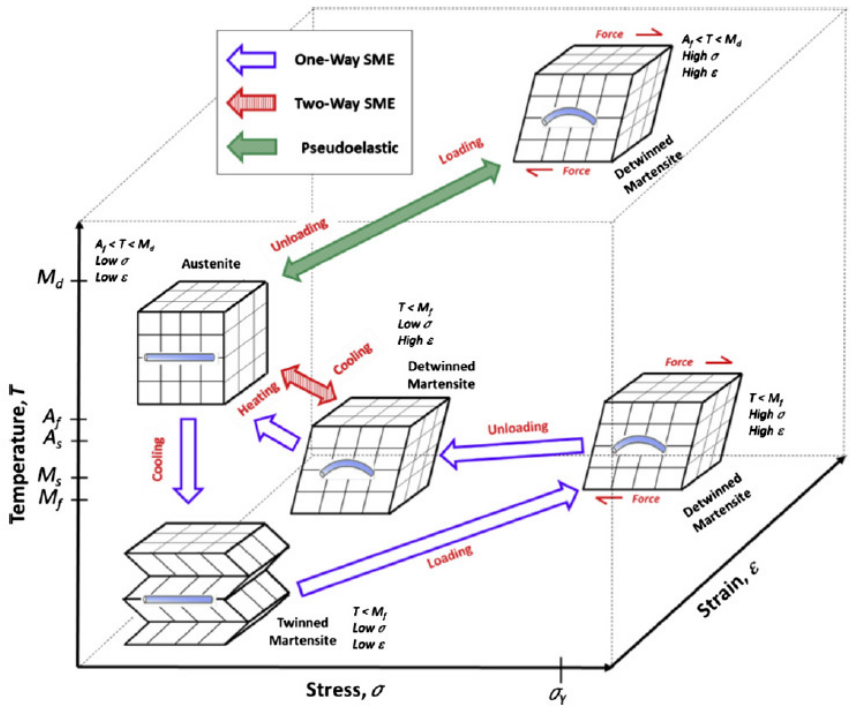

Figure 1.8: Phases and crystal structures in the shape memory alloys [4]

Figure shown below clearly illustrates the general schematic stress-temperature diagram of the shape memory alloys. At the higher temperatures than the austenite finish (A_f) temperature, the shape memory alloy is in the austenite phase, and below the martensite finish (M_f) temperature, the shape memory alloy (SMA) is in the martensite phase.

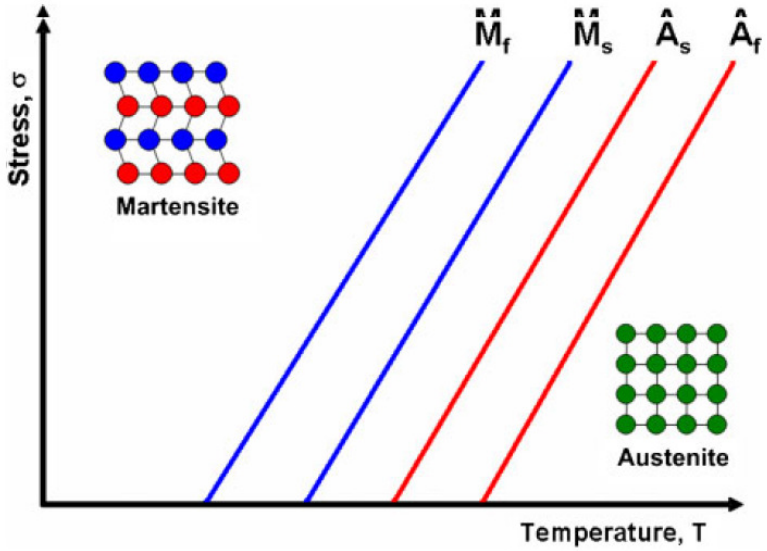

Figure 1.9: Stress-temperature diagram of shape memory alloys [5]

Figure given below illustrates the one-way shape memory effect in the stress-strain graph in the alloys. In general, de-twinning and the reorientation behaviours are important in the shape memory alloys [5].

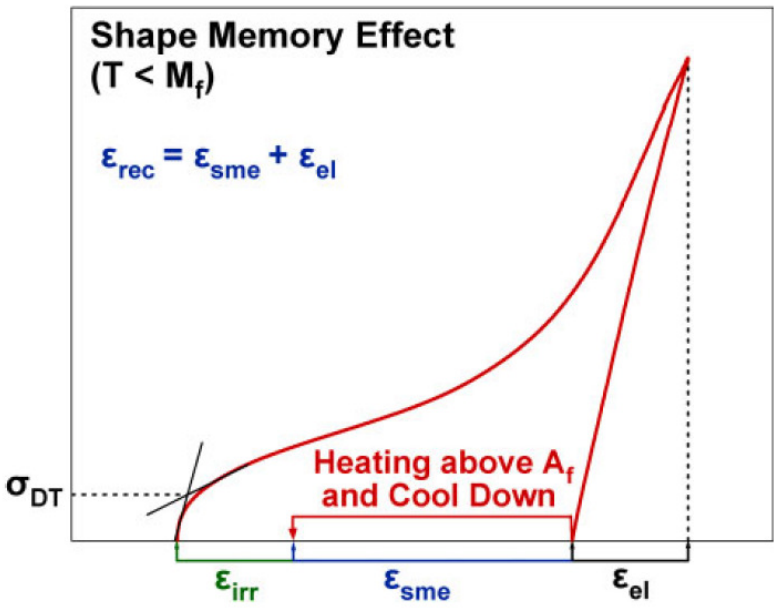

Figure 1.10: One-way shape memory effect [5]

Superelasticity (Pseudoelasticity)

Superelasticity (pseudoelasticity) is a type of shape memory alloy. Superelasticity (pseudoelasticity) can be attributed to the stress-induced transformations.

Superelasticity (SE) is the return of the strains (deformations) for the stress-induced martensite at temperatures higher than austenite finish (A_f) upon unloading.

In general, martensitic transformation is a shear-likeprocess. Stress assists the transformation of the martensite, and above martensite start (Ms) temperature, formation of the martensite phase is possible by using of force (load). This type of martensite can be described as stress-induced martensite.

Figure given below illustrates the superelasticity (pseudoelasticity) behaviour in stress-strain diagram of the shape memory alloys. σ_{SIM} is the critical stress value for the martensitic transformation. ε (strain) values (irr, se and el) are the irrecoverable strain (irr), superelastic shape strain (se) and the elastic strain (el).

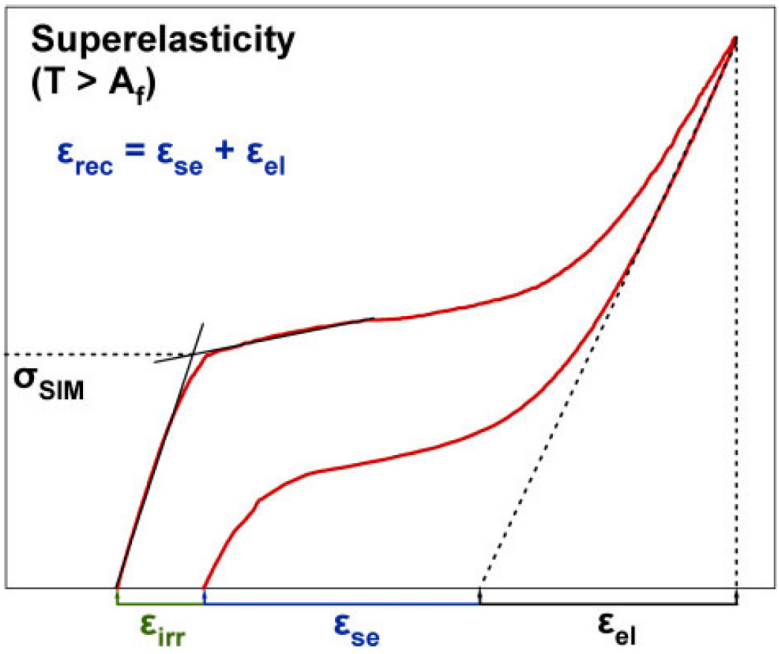

Figure 1.11: Superelastic properties [5]

Table 1.1 given below provides a general summary and several examples for the metal based, polymer based and ceramic based shape memory materials.

Table 1.1: Shape memory materials [4]

Materials	Examples	Notes
Metals	SMA: • NiTi-based alloys: NiTi, NiTiCu, NiTiPd, NiTiFe, NiTiNb, NiFeGa, NiTiCo • Cu-based alloys: CuZn, CuZnAl, CuAlNi, CuAlNiMn, CuSn ... • Fe-based alloys: FePt, FeMnSi, FeNiC ... • Ag-based alloys: AgCd ... • Au-based alloys: AuCd ... • Co-based alloys: CoNiAl... MSMA/FSMA: NiMnGa, FePd, NiMnAl, FePt, Dy, Tb, LaSrCuO, ReCu, NiMnIn, CoNiGa...	The best choice is NiTi SMA E.g. NiTi-based: Frequency: ⩽3 Hz, dia. 100 μm with natural cooling (Very Slow).Strain: max. 10% (High), Recommended: 4%.Stress: up to 500 MPa (High), Recommended: 100 MPa.Max. operating temp: ca. 100 °C (Low). E.g. NiMnGa: Frequency: max. 2 kHz (High), Recommended: 500 Hz Strain: max. 10% (High), Typical: 6% Stress: max. 9 MPa (Low), Typical: 3.4 MPa Young modulus: 0.5 GPa (Very Low) Max. operating temp: 72 °C. (Low), full austenite transition at 48 °C.
	HTSMA: TiNiPd, TiNiPt, NiTiHf, NiTiZr, ZrRh, ZrCu, ZrCuNiCo, ZrCuNiCoTi, TiMo, TiNb, TiTa, TiAu, UNb, TaRu, NbRu, FeMnSi and etc.	So far, TiNiPd and TiNiPt produced the best results and commercially ready E.g. TiNiPd Frequency: <1 Hz with natural cooling (Very Slow) Strain: 1.5–4.0% (Med) Stress: max. 295 MPa (High) Max. operating temp: 83–513 °C (Very high)
Polymers	PTFE, PU, Poly-caprolactone, EVA + nitrile rubber, PE, Poly-cyclooctene, PCO–CPE blend, PCL–BA copolymer, Poly(ODVE)-co-BA, EVA + CSM, PMMA, Copolyesters, PET-PEG ...	E.g. PU-based: Frequency: max 1 Hz (Very Slow) Strain: >800% (Very High) Stress: 3 MPa (Low)
Ceramics	ZrO_2 (PSZ), MgO, CeO_2, PLZT, PNZST ...	Shape memory ceramics has limited shape memory effect (below 0.5 %) E.g. PNZST: Frequency: ca. 1 kHz (High) Strain: <1% (Very low) Stress: max. 100 MPa (High), Typically: 35 MPa. Operating temp: 200–500 °C (Very high).
Others	SMM thin film: NiTi, SMP and etc.	This technology is based on smart materials applied to a thin film to produce SME for MEMS applications E.g. NiTi-based: Frequency: <100 Hz (Med) Strain: max. 10% (High), Typically: 7%. Stress: up to 500 MPa (High), Recommended: 100–350 MPa. Max. operating temp: ca. 100 °C (Low).

Nitinol (Ni-Ti)

Nitinol is a very popular material in the several engineering applications. In general, nitinol (Ni-Ti alloys) shows shape memory effect and superelasticity (pseudoelasticity) effect. Usually, nitinol includes nickel (Ni) and titanium (Ti) elements at the equal atomic percentage.

In general, the unique and usefull engineering properties of the nitinol shape memory materials are attributed to their reversble martensitic phase transformation behaviours.

The manufacturing process of the nitinol (Ni-Ti) is very difficult. Chemical composition of the nitinol must be controlled very tightly. Heat treatment process of the Ni-Ti is also very important. Several usefull engineering properties of the Ni-Ti can be controlled by aging heat treatment and subsequent cold working process.

In the biomedical applications, a stent is a metal based or plastic based simple tube, which put into a lumen of an vessel (arter or vein) to keep the artery open.

Table 1.2: Properties of the NiTi [4]

Property	Symbol	Units	Value	
			Martensite	Austenite
Corrosion Resistance	–	–	Similar to 300 series SS or Ti-alloy	
Density	ρ_D	kg/m^3	6450–6500	
Electrical Resistivity (approx.)	ρ_R	μΩ cm	76–80	82–100
Specific Heat Capacity	c	J/kg K	836.8	836.8
Thermal Conductivity	k	W/m K	8.6–10	18
Thermal Expansion Coefficient	α	m/m K^{-1}	6.6×10^{-6}	11.0×10^{-6}
Ultimate Tensile Strength	σ_{UTS}	MPa	895 (Fully annealed)/1900 (Hardened)	
Young's Modulus (approx.)	E	GPa	28–41	75–83
Yield Strength	σ_Y	MPa	70–140	195–690
Poisson's Ratio	ν	–	0.33	
Magnetic Susceptibility	χ	μemu g	2.5	3.8

Shape Memory Polymers

In the shape memory polymers, general mechanism for the shape memory can be attributed to 2 phase structure.

- Fixing phase (hard segment), which can return the permanent shape.
- Reversible phase (soft segment), which can fix the temporary shape.

In general, chemical crosslinks (covalent bonds) and physical crosslinks construct the hard phase. Physical crosslinks can be seen in polymers with crystalline and amorphous regions. Figure shown below illustrates the general shape memory mechanism in the polymers [1]

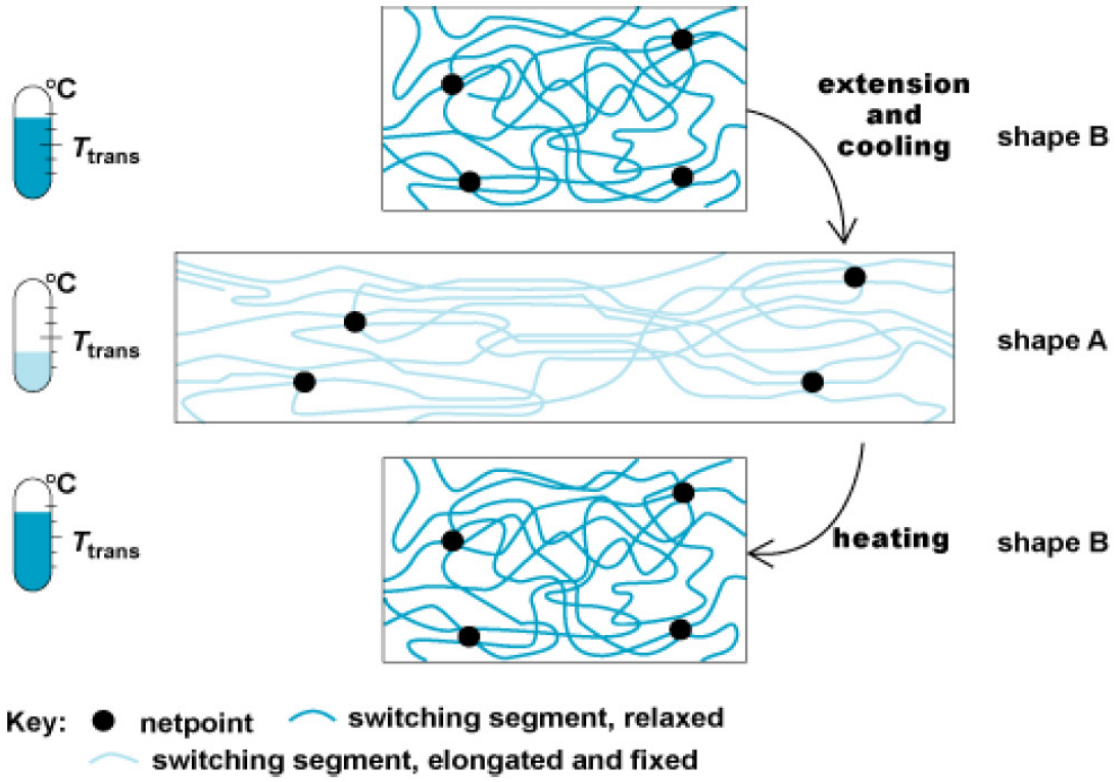

Figure 1.12: Shape memory mechanism in polymers [1]

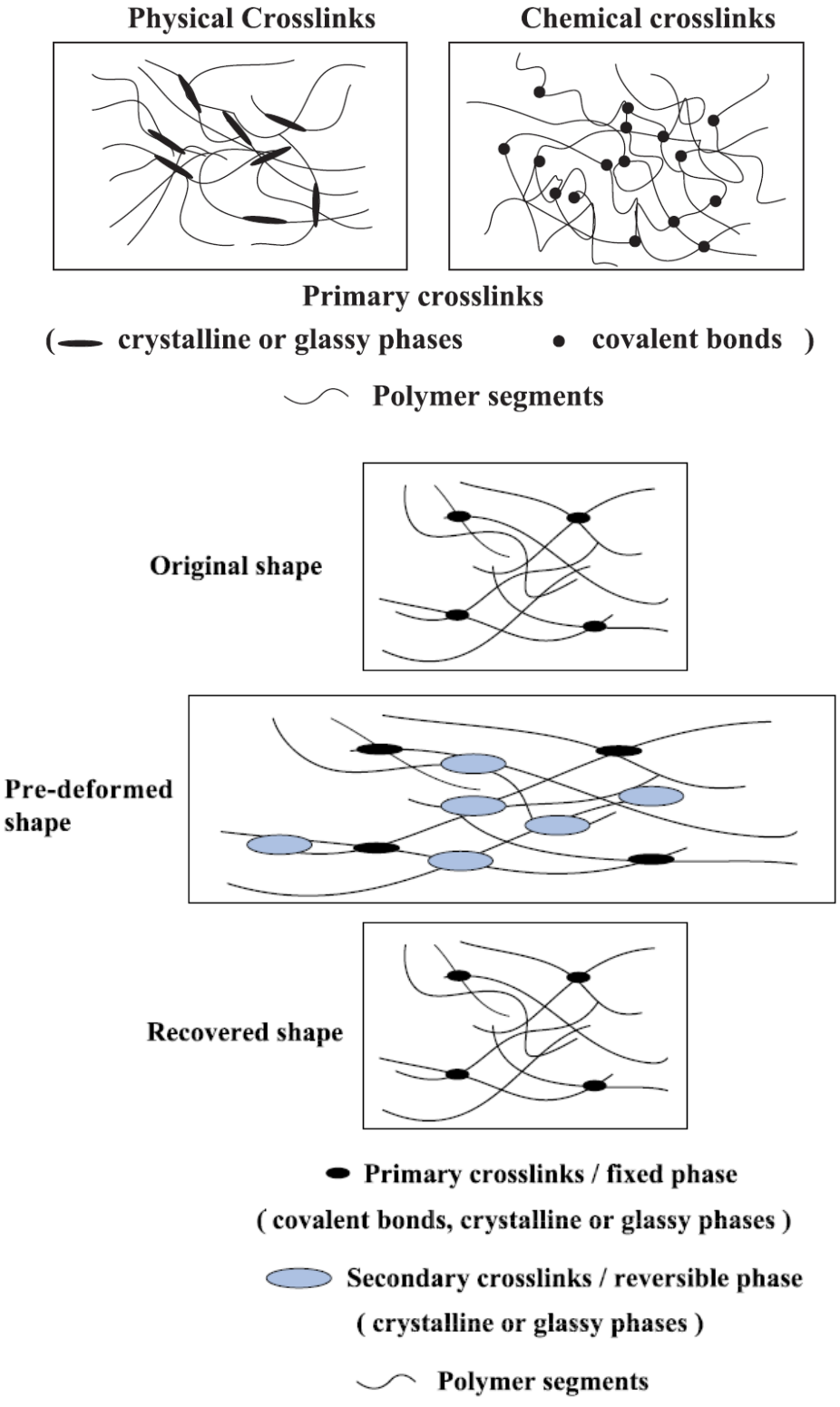

Figure 1.13: Shape memory polymers [6]

1.4. SELF HEALING MATERIALS

In general, the self-healing (SH) behavior can be defined as the capacity of a group of material to heal (repair) the defects (micro-cracks, micro-pores).

- Autonom type SH (without any intervention)
- Automatic/Nonautonom type SH (needs human intervention/external triggering)

In the autonom (without any intervention) self-healing property, there is no need to additional stimulation to trigger the healing. In the non-autonomic (human intervention/external triggering) self-healing property, an external effect (heat, light, or electricity) is needed after the defect formation.

Self-healing (SH) properties

- Extrinsic type SH (added)
- Intrinsic type SH

Self-healing (SH) of the extrinsic type materials is depends on the external healing materials. Specific healing materials must be included into the polymer main phase as a capsules, fibers, or networks. After the formation of the defects in the material, release (autonomous) of the healing materials starts the self-healing process.

For the intrinsic healing, there is no any healing materials. Moreover, the healing behavior attributed to the properties of the material.

General Classification of the Self-Healing (SH) Mechanisms

- Microcapsules based
- Hollow Fibers based
- Microvascular Network based

Figure shown below illustrates the self-healing behaviours of the polymers by using embedded healing materials into the matrix. There is a capsulation of the self healing materials (liquid resins or monomers) in hollow fibers in the type A. There is microcapsules in the type B. The type C illustrates the vascular network type self-healing. In the type D there is a paramagnetic nanoparticles for the healing [7].

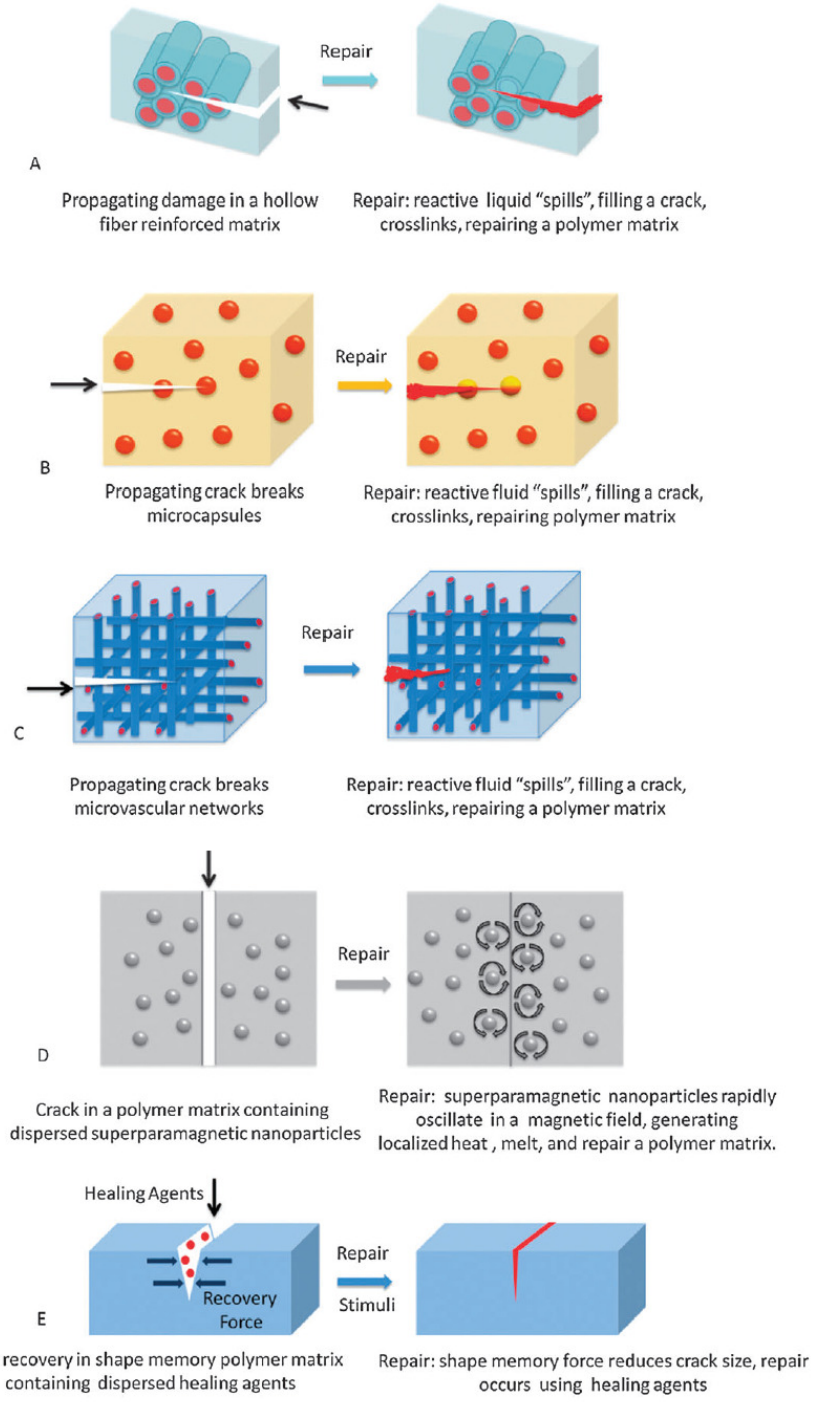

Figure 1.14: Self-healing of the polymers [7]

1.5. CORONARY STENTS

In general, a medical stent is a very small hollow tube-shaped device. Stents can be employed in the angioplasty applications to open the blocked veins or to improve blood flow in the arters of the human heart. In addition, stents can be used in the other parts of the body (peripheral stents). The coronary stents are generaly produced from specific metal alloys. Usually the coronary stents are coated with a very thin specific medicines (drug) that released in a controlled rate into the blood. These drugs can stop the arters from blocking again [8-11].

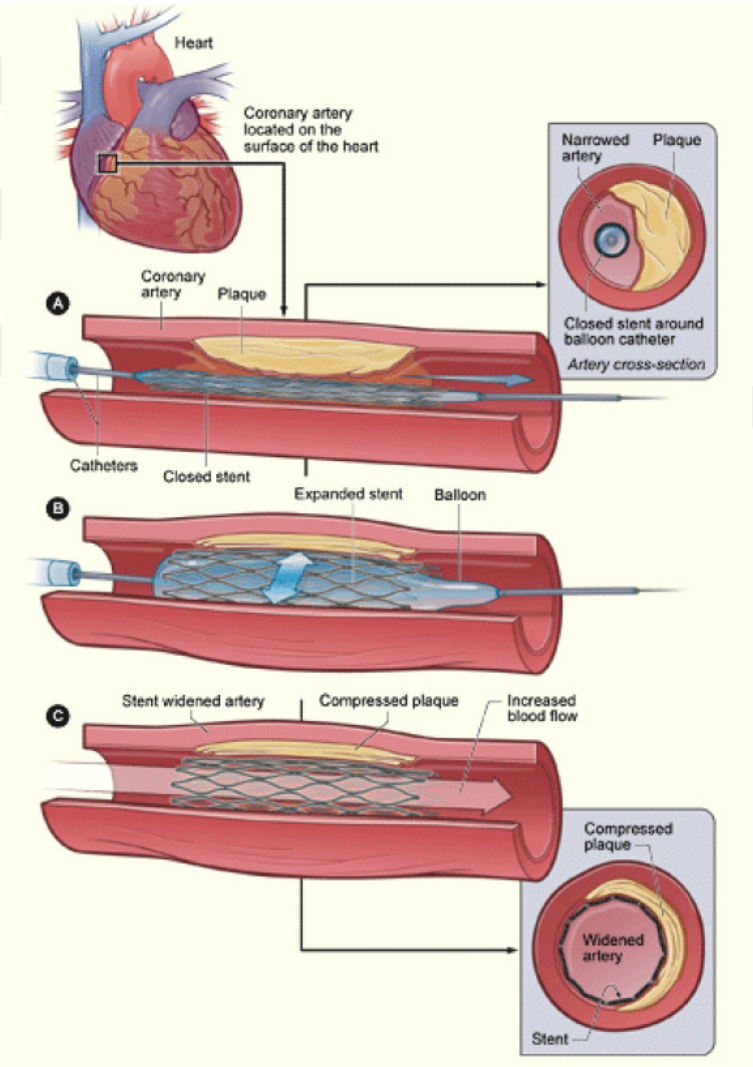

Figure 1.15: Placement of a stent [8]

The SEM images of the main production steps of a coronary stent. First, a mini-tube production, Then, in the second step, laser-cut of the mini-tube. Then, annealing and laser cuting of the minitube. Lastly, descaling and finishing of the coronary stent. Also there are reservoirs on the surface of the stents for the drugs.

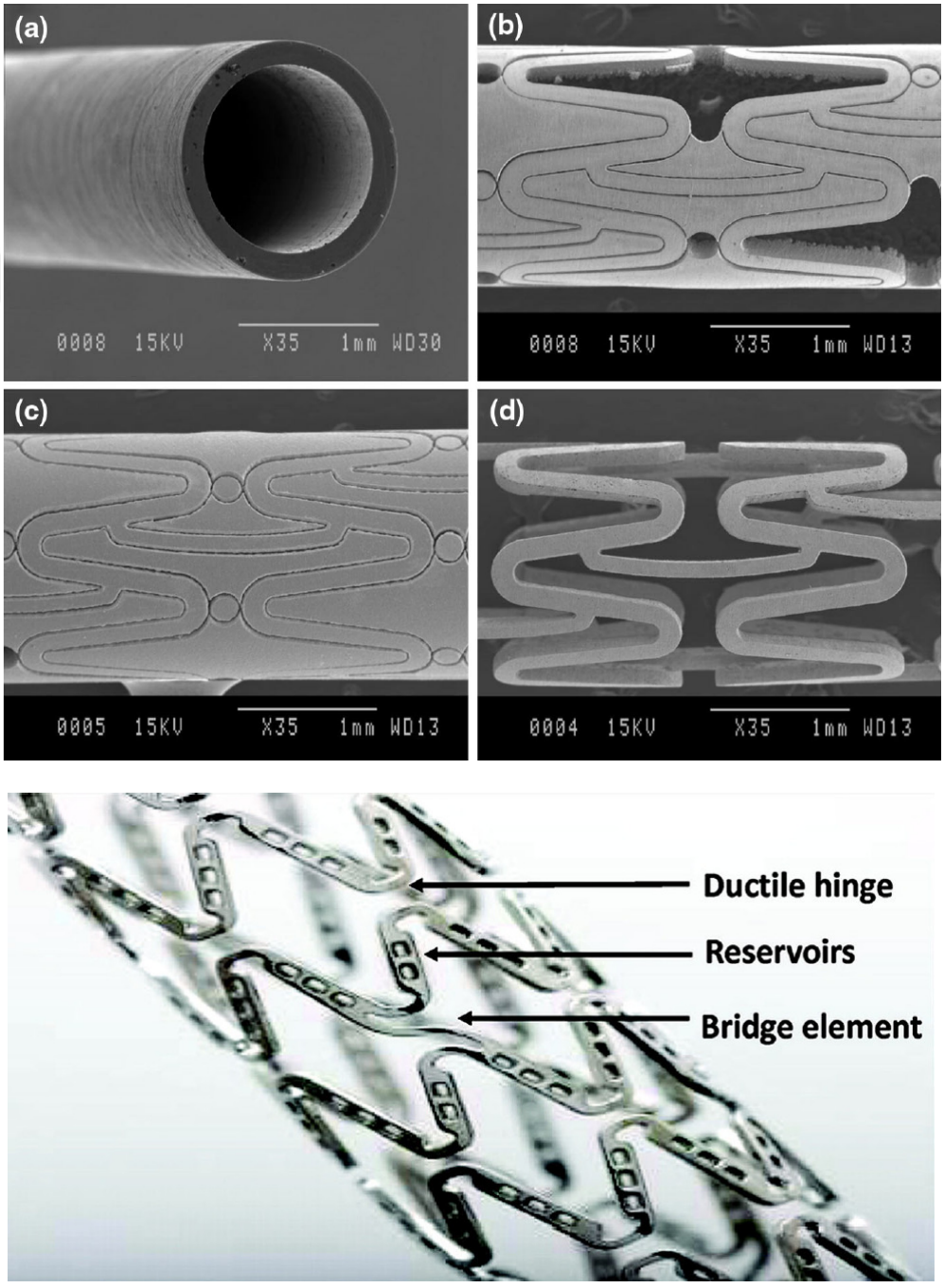

Figure 1.16: Production steps of a stent [9]

1.6. RAPID PROTOTYPING

In general, additive (layered) manufacturing (AM) is a layer-based manufacturing method that are employed to produce 3-dimensional physical products from 3-dimensional digital geometry data (CAD) as an input. Rapid prototyping (RP) is a engineering manufacturing method for the production of the several products (prototypes) from a CAD dfileata. In general, prototype is an early test specimen (model) of a product. In the rapid prototyping (RP), the product (prototype) is layered and the manufacturing is done by layer by layer.

Main advantages

- Cheaper method i some cases
- When you need 1-2 specimens, traditional methods are expensive
- Prototype can be used as a model in “investment casting”
- You can check the prototype (mechanical and visual control)
- Complex parts can be produced
- Mechanisms could be checked
- You can chec the modular parts (check the function of the each part in the assembly)

Main disadvantages

- Surface flatness is rough (dependant of material and type of RP)
- Brittle material

Main steps of the rapid prototyping methods (additive manufactirng)

- Creation/drawing/scanning of the CAD model of the product
- Transformation/convertion of the CAD file into the STL (stereolithography) file
- Determination of the Z-axis of the product
- Layering (slice the STL file into controlled number of layers)
- Manufacturing of the product (printing)
- Removing of the supports/scaffolds from the surface of the product
- Cleaning and finishing

As shown in the figure given below, vat photopolymerisation technique employs a vat of a liquid photo-polymer as a raw material, which the prototype is manufactured layer by layer. UV light is employed for curing (solification) of the photopolymers resins.

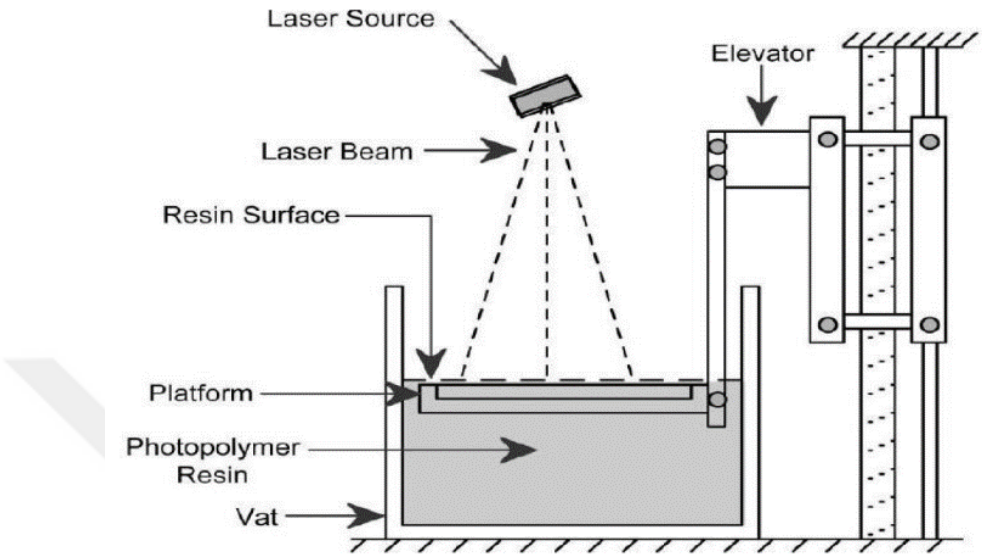

Figure 1.17: Photo-polymerization method [12]

Figure given below illustrates the fused deposition modelling (FDM) technique. In general, two types of raw materials can be employed in the FDM devices. Modeling material and a support (scaffold) material, which is removed from the surface of the product (prototype) after the printing process.

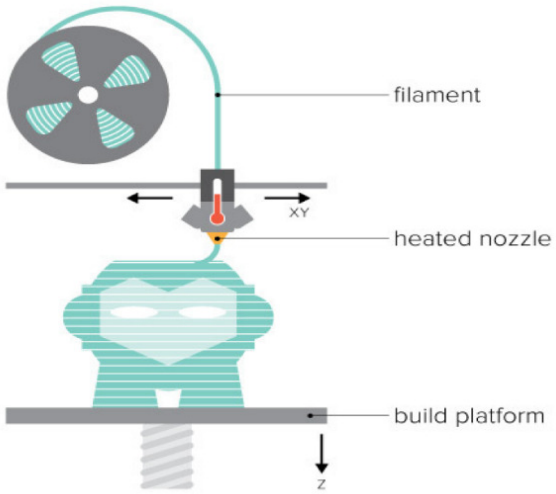

Figure 1.18: Fused deposition modelling (FDM) method [12]

In general, selective laser sintering (SLS) technique is is a laser beam-based method that uses metal powder as a raw material. A laser beam sinter together the metal particles in the bed, by heating the metal powder temperature.

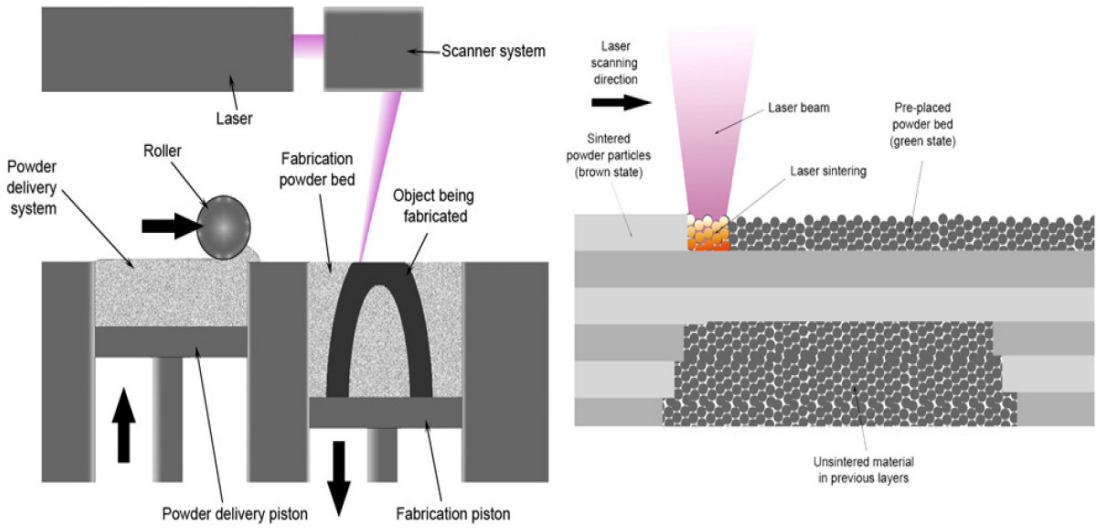

Figure 1.19: Selective laser sintering (SLS) method [12]

Electron-beam melting (EBM) is a type of 3-dimensional printing method especially for the metal based products. EBM (electron-beam melting) is a powder-based (metal or ceramic) sintering method. Electron-beam melting (EBM) employs a very narrow electron beam, which having high energy and very narrow diameter.

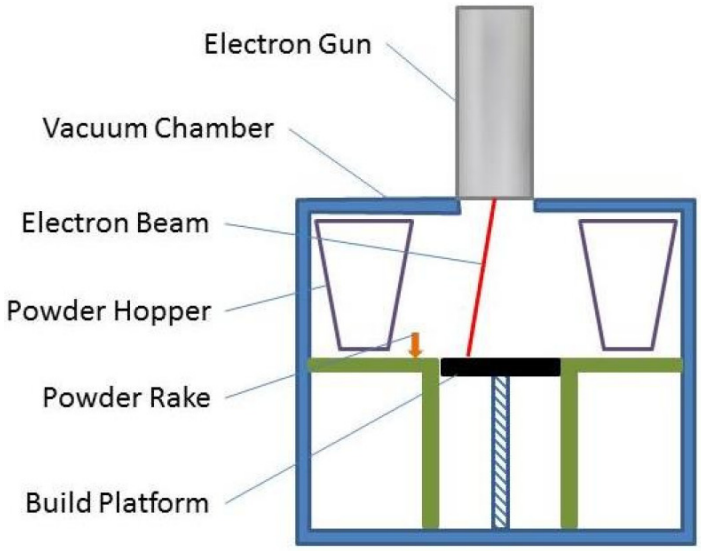

Figure 1.20: Electron beam melting (EBM) method [12]

Figure shown bellow clearly illustrates the classification of the additive manufacturing method according to type of their raw materials. There are liquid based (resins or monomers), solid based (polymer flament) or powder based (metal, ceramic or polymer) methods. In addition, additive methods can be classified according to sintering (solidification) mechanism, such as electron beam, laser beam, UV [13].

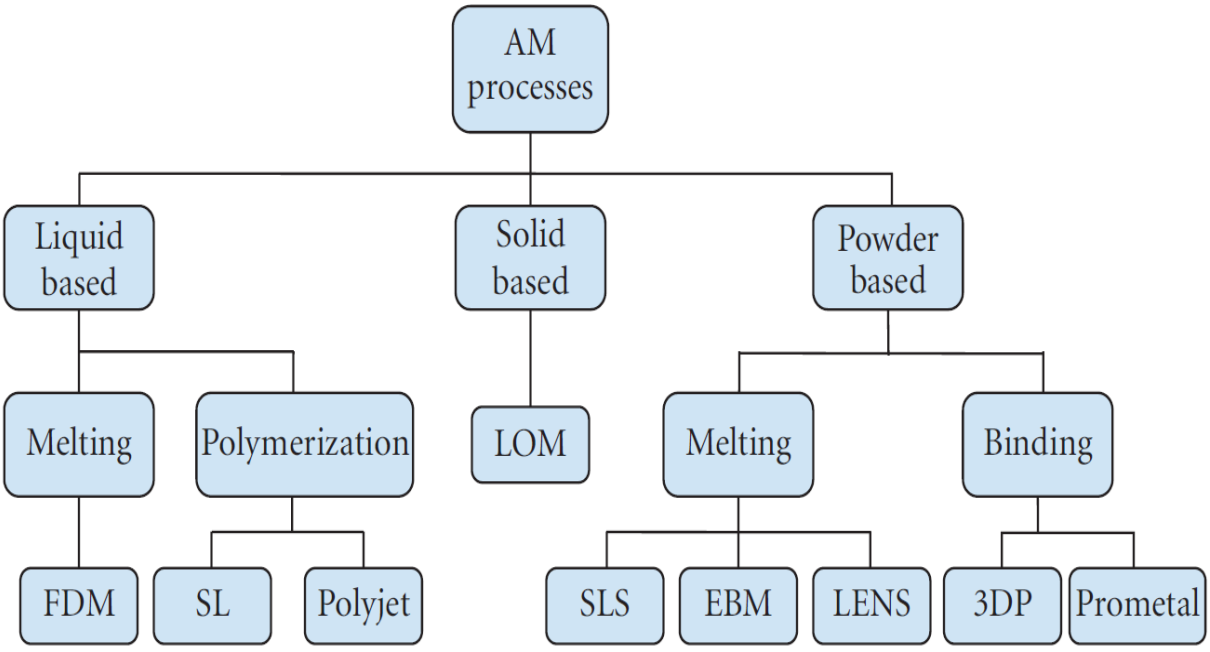

Figure 1.21: Classification of the additive manufacturing method [13]

1.7. POWDER METALLURGY

In general, powder metallurgy (PM) manufacturing methods can be classified into two main groups: traditional pressing-sintering based methods and advanced methods (full-density processes). Several powder ingredients can be employed to enhance the process parameters and meet the needs of the final product. For example, in cold pressing irregular powders are employed to ensure high green strength and structural integrity of the compacted product. Special solid lubricants can be added to the powder mixtures to lower the friction between the metal particles and the die wall [14-16].

General advantages of the powder metallurgy (PM)

- Unlimited choice of alloys (wide solubility range)
- Composite materials (metal matrix composites) can be produced
- Refractory metals, with high melting temperatures, can be shaped
- Controlled porosity for self lubrication or filtration
- Cheaper at large product numbers
- Close control of the dimensions
- Near-net shape

Disadvantages of the powder metallurgy (PM)

- Limited product dimensions
- Special machines
- Need to control the environment - corrosion concern
- Lower mechanical properties than the wrought materials.
- Expensive machines and dies
- Cost of the metal powders

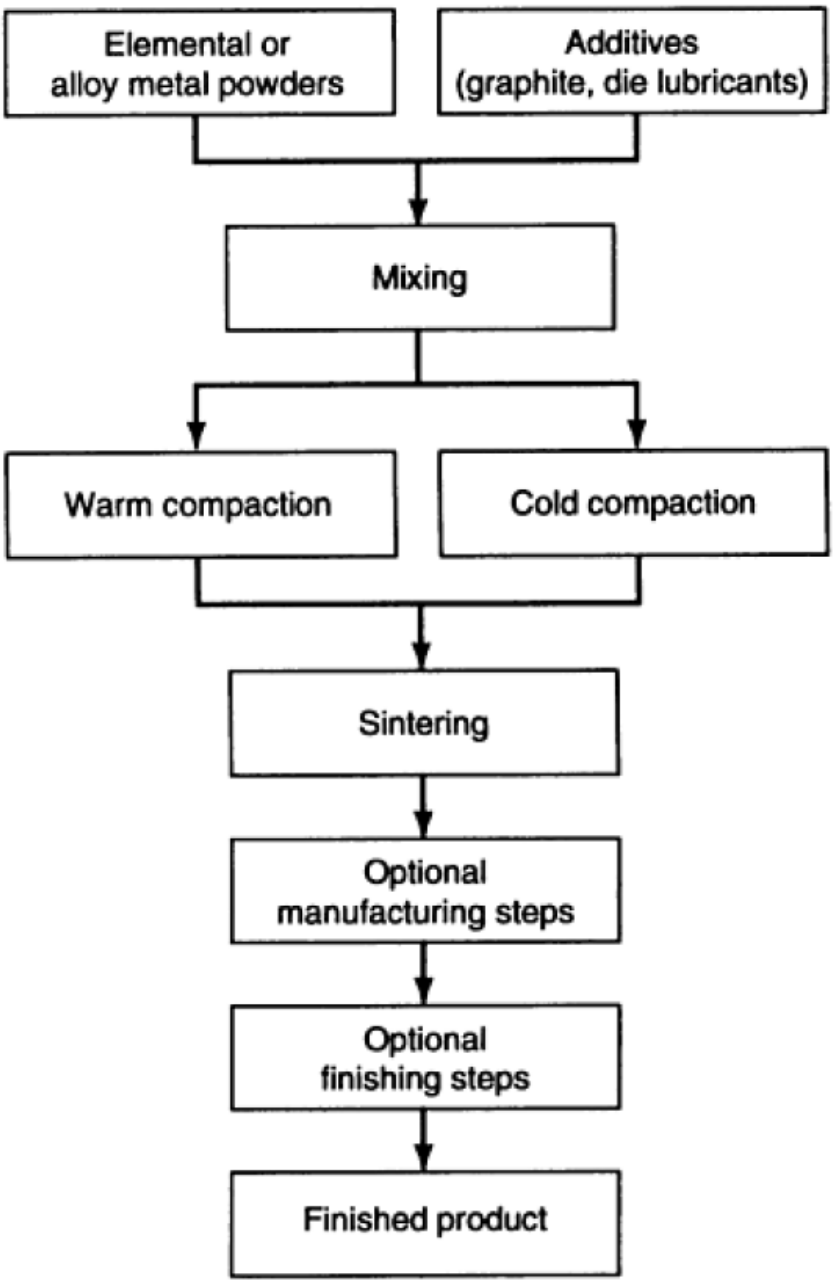

Figure 1.22: Main steps of the powder metallurgy method [16]

1.8. LITERATURE REVIEW

Yuan et al. [17] were studied 3-dimensional printed mechanical metamaterials with high energy absorbtion. 3-dimensional metamaterials can be obtained by inaccessible mechanical properties in natural materials. Metamaterials show egative Poisson's ratio, and thermal expansion coefficient. The authors, produced carbon nanotubes reinforced nanocomposite auxetic (metamaterial) specimens produced by selective laser sintering showing impact energy absorption capacity. Optimization of the several parameters was provided the enhancement of the impact energy absorption capacity of the auxetic metamaterials. Auxetic materials were provided high energy absorption capacity.

Wang et al. [18] were studied 2-dimensional mechanical metamaterials (auxetics). Auxetic materials (negative Poisson's ratio materials) show elastic properties in the orthogonal direction to the force. Auxetic materials shrink when compressed and expand when stretched. This geometry can obtain higher negative Poisson's ratio. The metamaterials (auxetics) with unit cells with peanut-shaped holes are manufactured by rapid prototyping (RP). Experiments were conducted to show the auxetic metamaterial behaviour. Effects of the parameters on the Poisson's ratio were studied.

Jabur et al. [19] were studied the shape memory Ni-Ti alloys produced by powder metallurgy (PM) route. In this research, effect of the pressing pressure and additions of the Cr and Al on the mechanical properties of the specimens. Pressing pressure and Cr/Al additions were showed very low effects on thehardness, transformation temperatures raised with increasing of Cr and Al additions, porosity contents lowred with raising of pressure and Cr and Al contents.

Eda et al. [20] were studied powder metallurgy (PM) based Co added Ti-Ni alloy specimens. Cobalt powder (about 2%) was included to the Ti-Ni specimens to enhance the mechanical properties. Powder metallurgy 1% cobalt added Ti-Ni alloys showed high shape recovery rate. Moreover the yield stress of alloys was constant. Cobalt (Co) solution amount had no effects on the amount and sizes of fine aging precipitates.

Liu et al. [21] were investigated the novel biodegradable Fe-Mn-Si shape memory alloys alloy. Microstructure, biocompatibility, mechanical properties (strength and elastic modulus), shape memory behaviour, electrochemical corrosion properties were experimentally studied. Strenth of the Fe-Mn-Si specimens was higher than that of the pure Fe, and the electrochemical corrosion rate of specimens was higher than Fe-Mn specimens. As a result, Fe-Mn-Si can be a alternative biomaterial with a shape memory behaviour.

2. MATERIALS AND METHODS

2.1. PRODUCTION OF POLYMER MATERIALS

Rapid Prototyping

In this thesis, the rapid prototyping (also known as additive manufacturing or 3-dimensional printing) route was employed in order to produce prototypes or products. In the present study, the prototypes were produced by a 3-dimensional printing device (Formlabs). 3-dimensional printing (rapid prototyping) device was stereolithography based (SLA). Photopolymer based liquid resin was used as a raw material. Prototypes were produced layer by layer by selectively photopolimerization (curing) of the liquid photopolymer resin using a UV light source. UV light was scanned by the mirror system to cure (solidify) the liquid polymer resin into hardened plastic part. SLA system was in upside-down (vertical) mode.

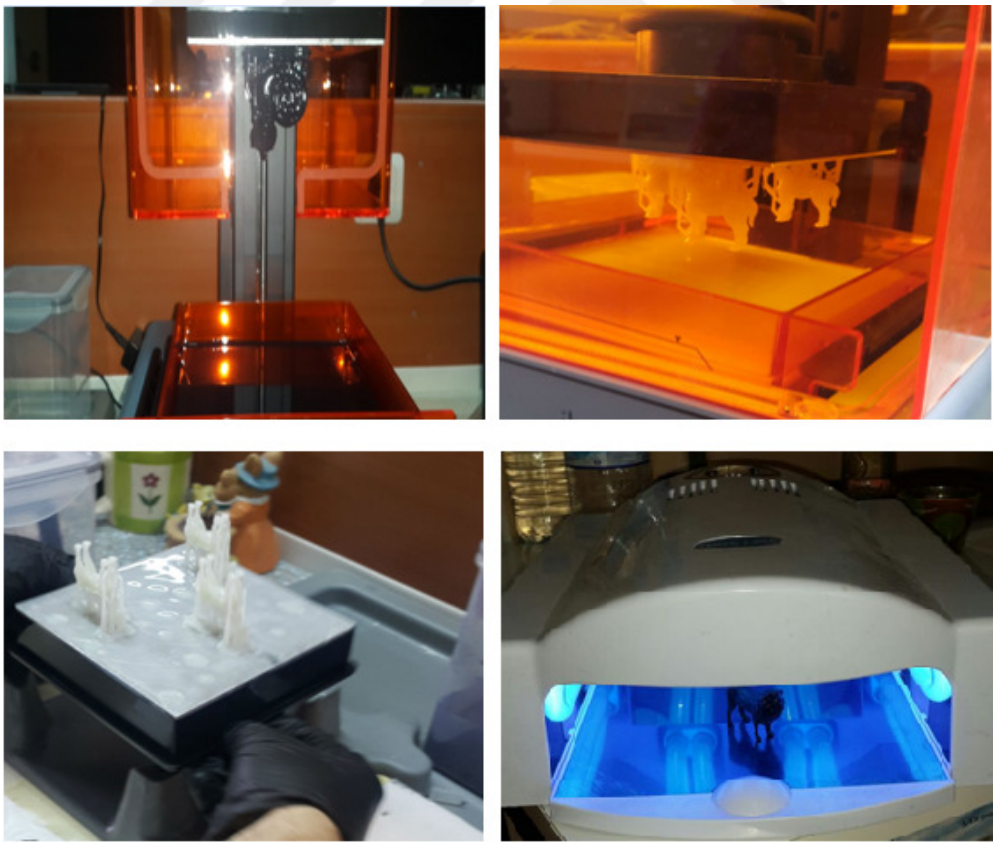

Figure 2.1: Stereolithography based rapid prototyping method

Replica Method

Impression moulding (alginate replica) method was employed for the production of the silicone based products. Elastic alginate was used as a moulding material (negative mould of the product). Alginate powder was mixed with water for the preparation of the mould. 2-component room temperature vulcanising (RTV) elastic silicone resin (polysiloxane) was poured into cavity of the alginate mould and then silicone products were produced. Liquid silicone was mixed with 3.0 % cross-linker before the casting step.

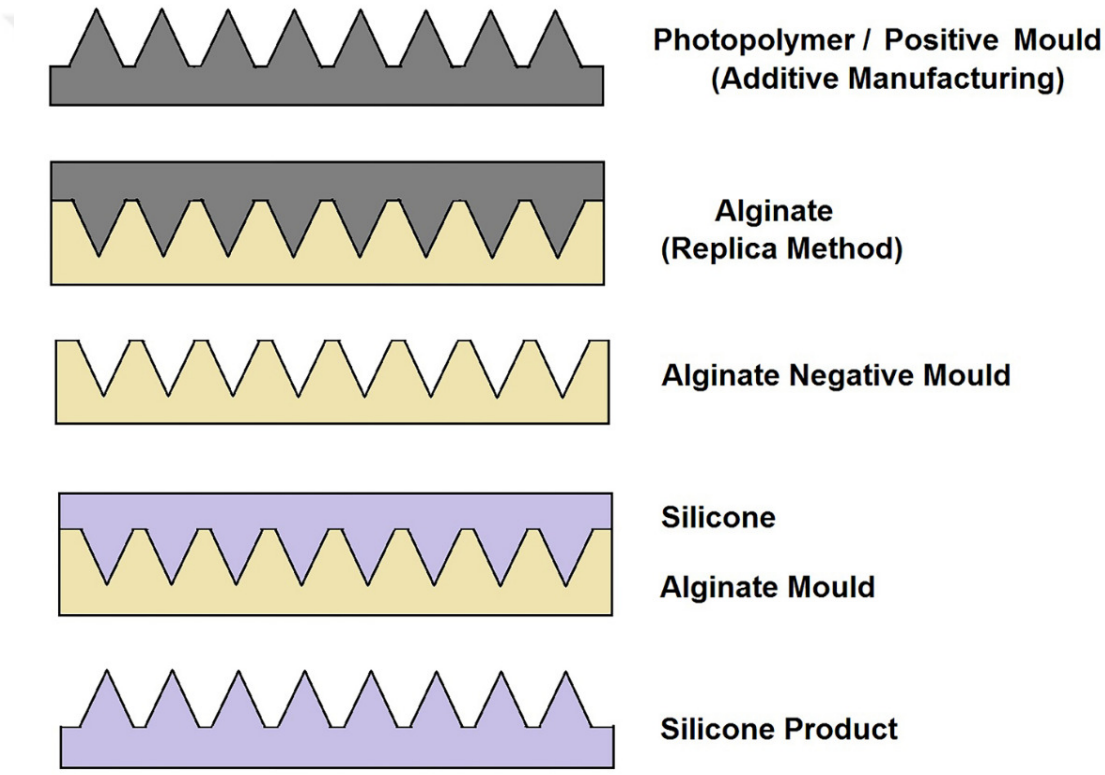

Figure 2.2: Replica method

Polyurethane Based Polymers Specimens

Figure given below illustrates the polyurethane (PU) polymerization mechanism and the polyurethane (PU) based specimens. Polyurethane (PU) specimens were produced by mixing the equal amounts of liquid polyol and liquid isocianate components, as shown below.

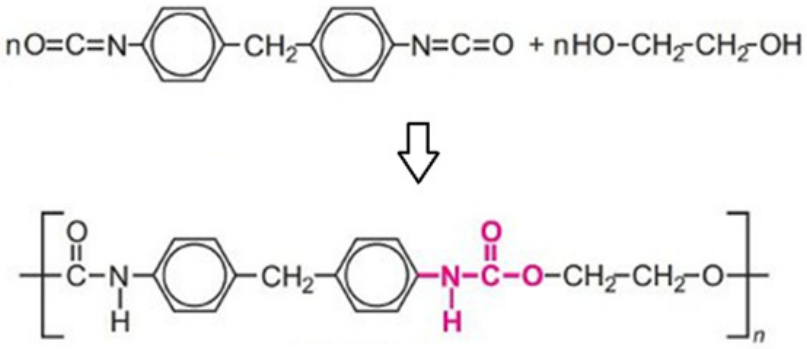

(a)



(b)

Figure 2.3: Polyurethane a) polymerisation mechanism and b) solid specimens

2.2. PRODUCTION OF METAL ALLOYS

Powder Metallurgy Method

In the experiments, the Ti-Ni, Ti-Ni-Sn, Ti-Ni-Co and Ti-Ni-Co-Sn based shape memory alloys were manufactured by using fine metal powders with average particle sizes of 30-40 μm (Alfa Aesar, USA). The Ti-Ni based green specimens were produced by the following steps: metal powder mixing step, alloy preparation by mechanical alloying (ball mill), and pressing step at about 200-50 MPa. Then, the sintering process of the green specimens at 1200 ºC was carried out under argon or vacuum atmosphere to prevent the oxidation of the alloys. Table given below shows the compositions of the Ti-Ni based shape memory alloys.

Table 2.1: Compositions of the Ti-Ni based alloys

Alloy	Co	Ni	Ti	Sn
Ti-Ni		50	50	
Ti-Ni-Sn		48-50	48-50	1-4
Ti-Ni-Co	1-4	48-50	48-50	
Ti-Ni-Co-Sn	1-4	48-50	48-50	1-4

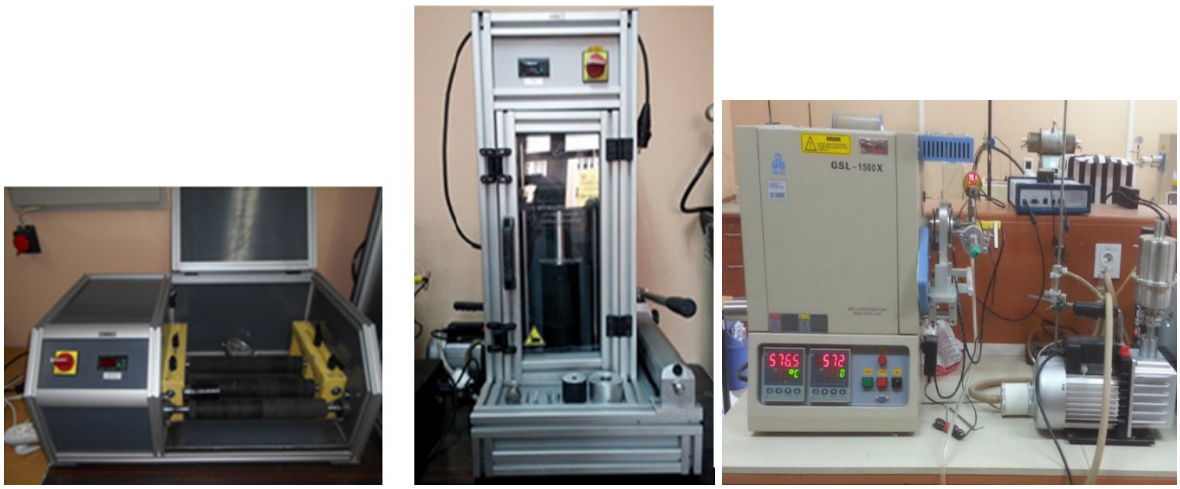

Figure 2.4: a) Ball mill and hydraulic press, b) sintering furnace

Powder Injection Moulding Method

In this method, rod shaped cylindrical product was manufactured by using fine metal powders (30-40 μm) using an injection-molding machine (MSE, Turkey). Polymer based binder system, which is important for mouldability/flowability, was consisted of 35-40 wt.% wax (paraffin), 60-65 wt. % polyethylene (PE). The final mixture was included plastic binder (35-40 %) and metal powders (60-65 %). Injection temperature of the process was 180-185 ºC. Polymers were removed by using heated hexane (for paraffin) and heating (for PE). Lastly, the samples were sintered at 1200 ºC.



Figure 2.5: Powder injection molding method

2.3. SHAPE MEMORY TRAINING

The sintering process was consisted of heating to 380 ºC (de-binding), then heating to the sintering temperatures. The green specimens were sintered at 1100-1200 ºC for 60 minutes. Sintering process was conducted in vacuum in a horizontal type tube furnace (MTI GSL1500X, USA). Then, the tube was removed out from the heating zone of the furnace, and metal samples were rapidly cooled directly from the sintering temperature at the cooling rate of 1.0-3.0 ºC/s. A cooling fan was employed at the end of the heating tube of the furnace. Subsequently, the metal specimens were precipitation hardened (aging) in the same furnace. The specimens were aged for about 60 minutes at 400 °C temperature.

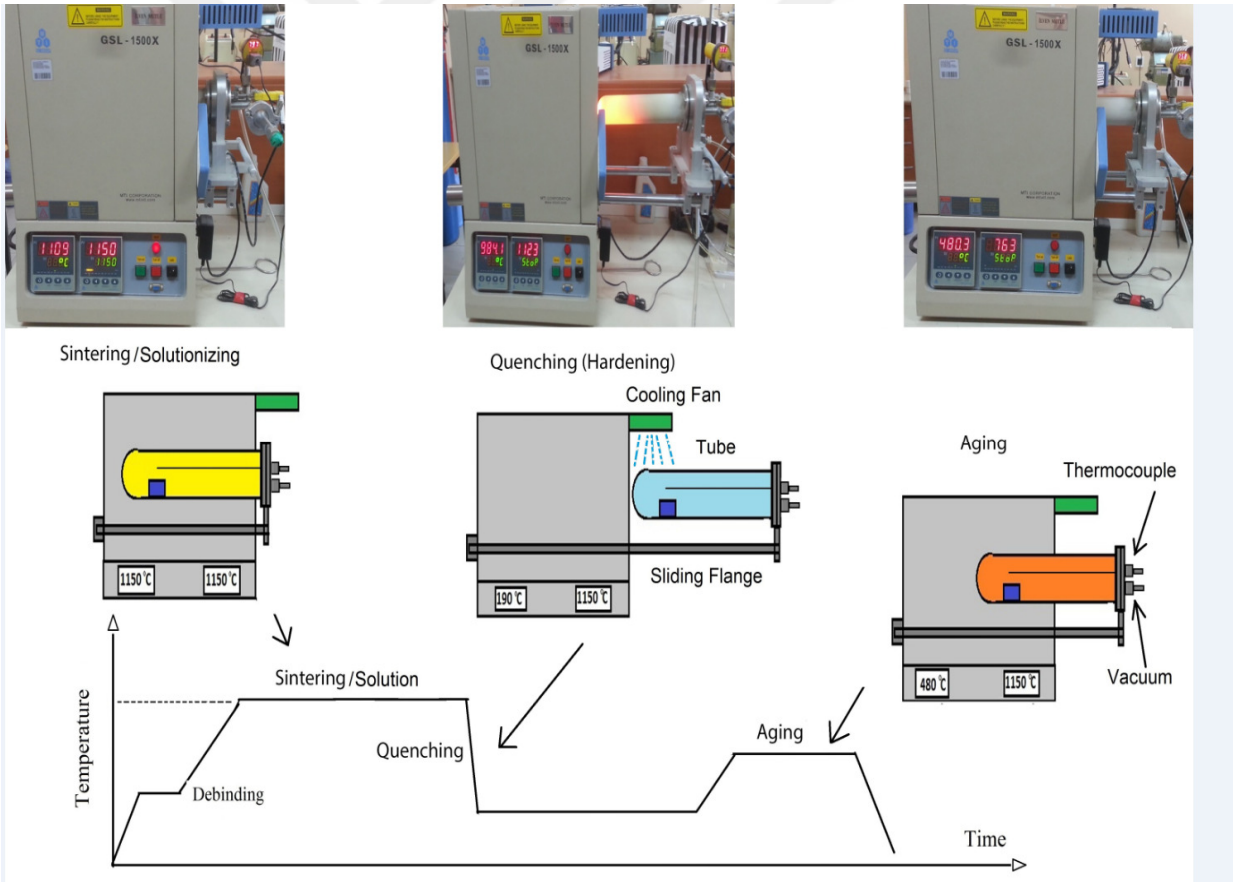

Figure 2.6: Shape memory training heat treatment

2.4. CHARACTERIZATION

2.4.1. Microstructure

The SEM (scanning electron microscope) device was used in order to investigate the microstructure (pore morphology, pore size and microstructural phases) of the specimens (FEI Quanta FEG 450). Densities (% porosity) were determined by using gravimetric (geometrical) method.

X-ray diffraction (Rigaku 2200) was employed for the identification and evaluation of the phases in the microstructure of the alloys.

Thermal behaviour of the PEEK was investigated by using differential thermal analysis (Seiko SII Exstar 6000 TG/DTA 6300, Japan).

Corrosion experiments were conducted in SBF (simulated (artificial) body fluid), which was produced in the light of the literature. The SBF was included (in g/L) of 8.00 NaCl, 0.4 KCl, 0.1 $CaCl_2$, 0.1 $MgCl_2$, 0.07 Na_2HPO_4, 0.07 Na_2SO_4, 0.70 $NaHCO_3$, and buffer (tris) (Merck). Electrochemical DC corrosion tests were performed using a potentiostat (Interface 1000, Gamry). Tafel curves were obtained in order to evaluate electrochemical corrosion behaviour of the specimens. Open circuit potential tests were carried out for 2 hours.

2.4.2. Mechanical Properties

Mechanical properties (Young's (elastic) modulus and strength) of the materials was examined by performing tension-compression tests (Devotrans, Turkey).



Figure 2.7: Tension-compression test device

Mechanical parameters of the alloys was also evaluated by non-destructive based ultrasonic testing (USM Go, General Electric). Measurements were carried out by pulse-echo mode transducer having 4 MHz probe [10-12].

$$E = \rho V_T^{\,2} \frac{3V^2_L - 4V_T^{\,2}}{V_L^{\,2} - V_T^{\,2}} \qquad (1)$$

3. RESULTS

3.1. POLYMER MATERIALS

3.1.1. Microstructure

Figure illustrates the pictures of the (a) acrylic based metamaterial prototype (mould), (b) negative alginate based mould, (c) polyurethane (PU) filled auxetic metamaterial.

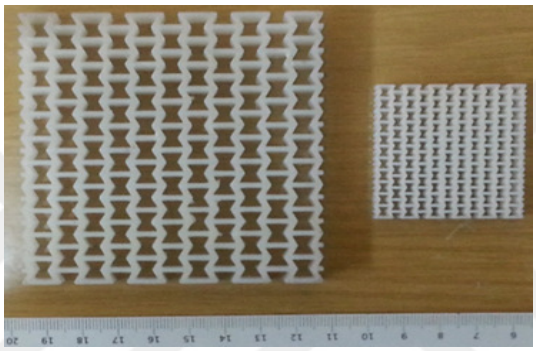

(a)



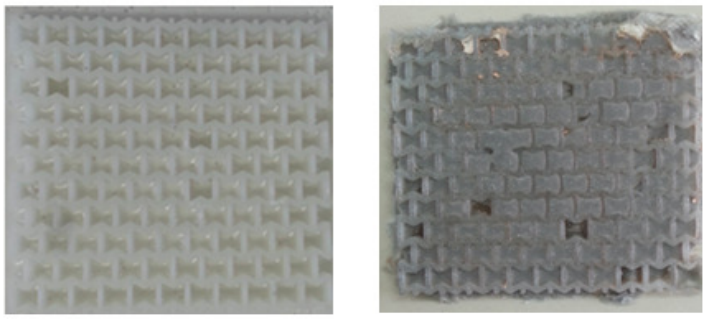

(c)

Figure 3.1: Pictures of a) metamaterial prototype, b) negative mould, c) filled metamaterial

Figure given below shows the SEM pictures of microstructure of (a) polyurethane (PU) matrix composite specimen, (b) silicone matrix specimen.

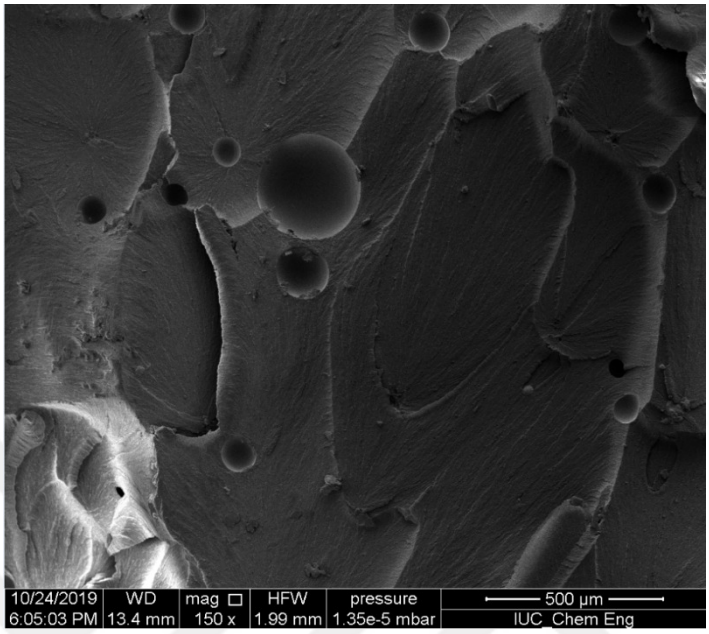

(a)

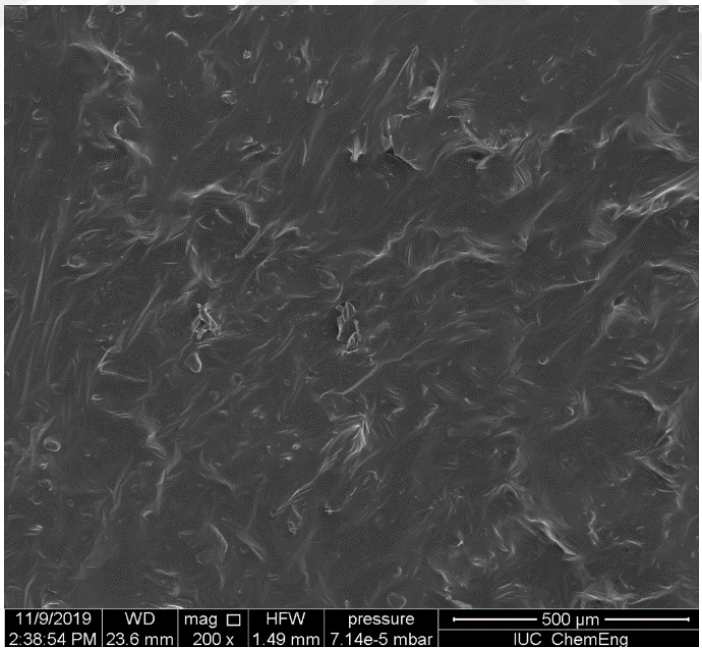

(b)

Figure 3.2: SEM pictures of microstructure of a) PU specimen, b) silicone specimen

3.1.2. Mechanical Properties

Figure given below illustrates the photographs during compression tests of the auxetic PU specimen (a) lateral (perpendicular) compression with respect to the re-entrant unit cell, and (b) vertical (axial) compression with respect to the re-entrant unit cell. Deformation mechanism of the auxetic polyurethane specimen was similar to the theoretical deformation of the auxetic meta-materials. Auxetic specimens were become denser with time. As the unit cell geometry is different with respect to applied force, lateral and vertical compression behaviours are different.

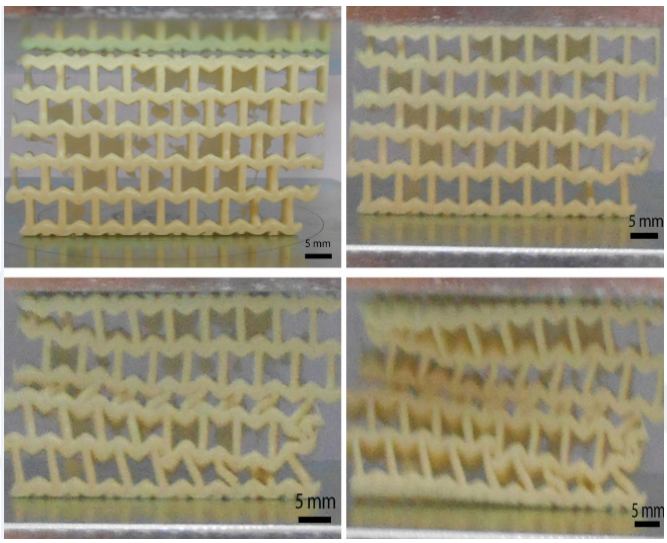

(a)

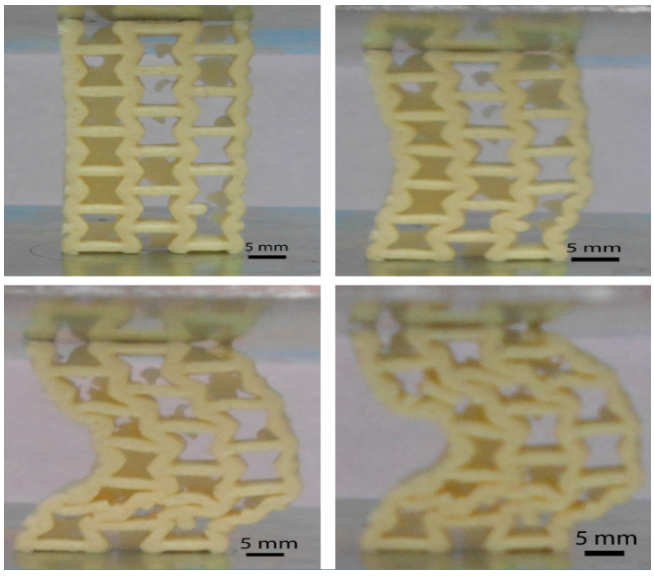

(b)

Figure 3.3: Photographs during compression tests of PU a) lateral, b) vertical

Figure given below illustrates the photographs during the compression tests of TiO_2 reinforced auxetic polyurethane matrix composite specimen (a) lateral (perpendicular) compression with respect to the re-entrant unit cell, and (b) vertical (axial) compression with respect to the re-entrant unit cell. Secimens were become denser with time. Deformation mechanism of TiO_2 reinforced auxetic PU specimen was similar to theoretical deformation of the auxetic meta-materials. As the unit cell geometry is different with respect to the applied force, lateral and vertical compression behaviours are different.

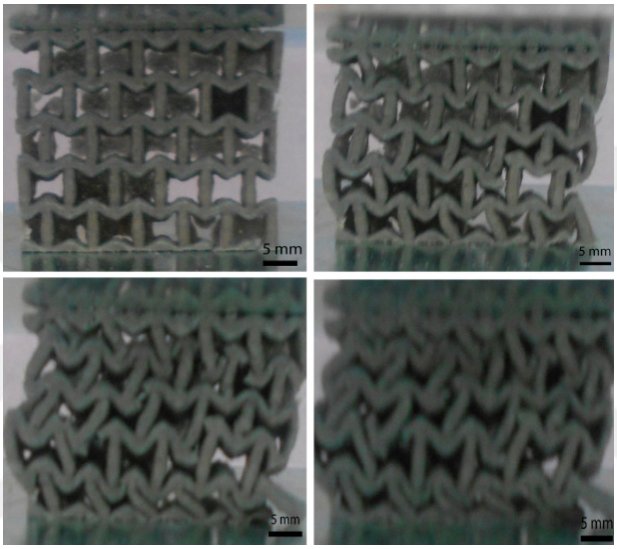

(a)

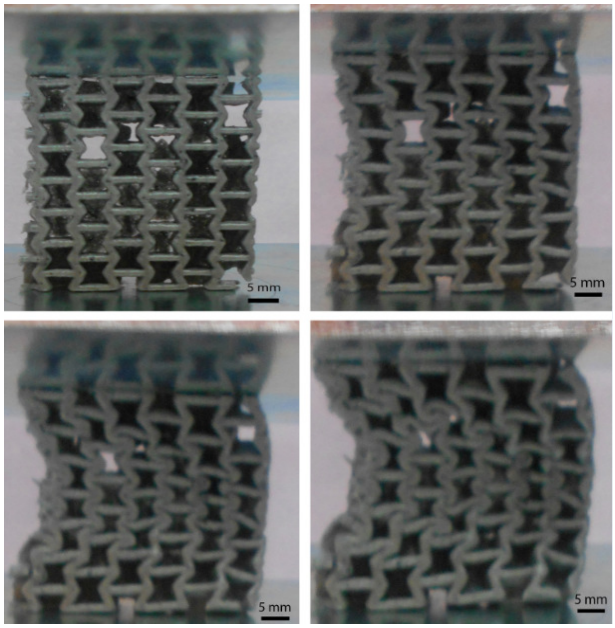

(b)

Figure 3.4: Photographs during compression tests of PU composites a) lateral, b) vertical

Figure given below shows the compressive stress-strain curves of the PU and TiO_2 reniforced auxetic PU composites. Mechanical properties (strength, elastic modulus) of the composite PU specimens were higher. Figure given below also shows, deformation mechanism of the re-entrant hexagonal star shape auxetic specimens, before-after loading, and schematic deformation mechanism of the unit cell. Deformation mechanism of the auxetic meta-material specimen was similar to the theoretical deformation of the auxetic meta-materials.

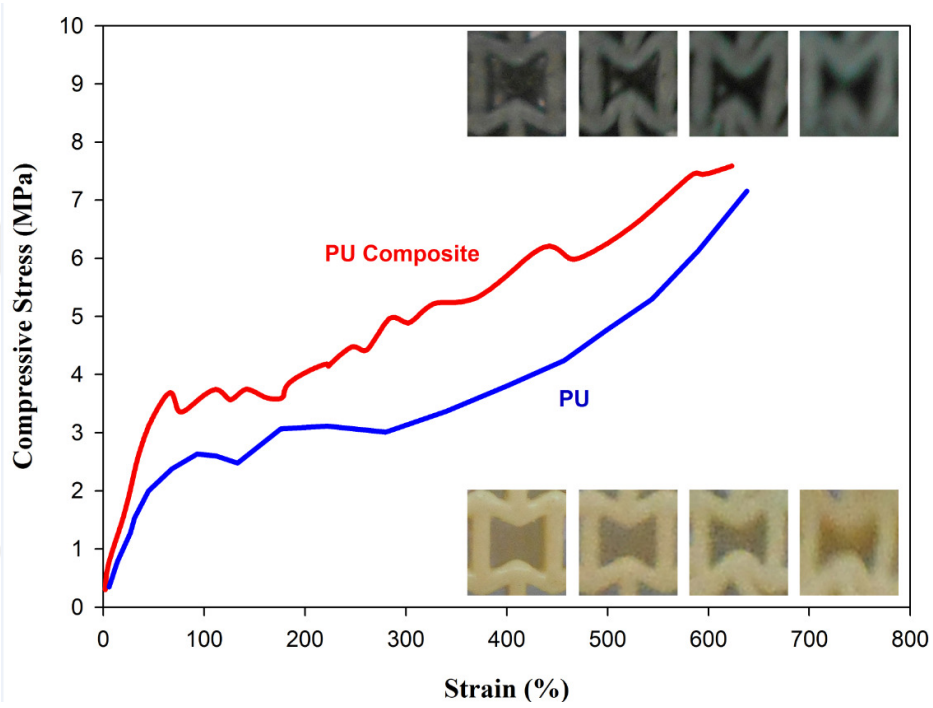

(a)

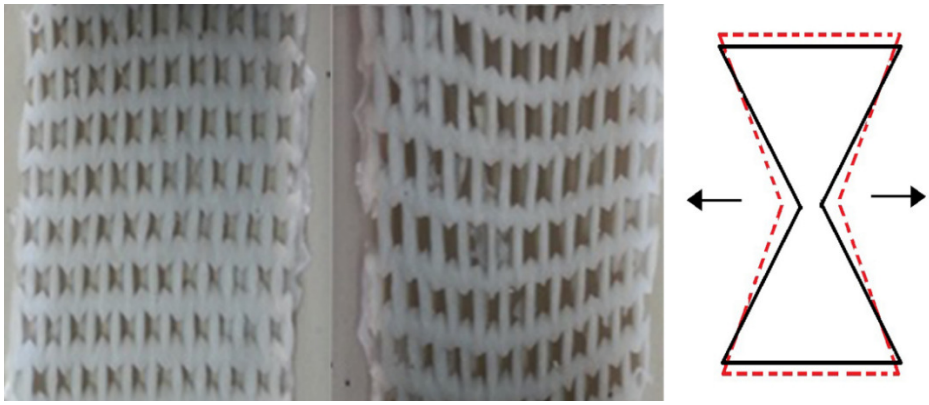

(b)

Figure 3.5: a) Stress-strain curves of the metamaterial PU, b) deformation mechanism

Figure given below shows the shape memory effect (SME) in the polyurethane (PU) based plate-shaped specimens. As shown in the figure, the PU based plate was remember its firs shape. In general, the amount of the recovery of the PU based plate was suitable for shape memory applications.

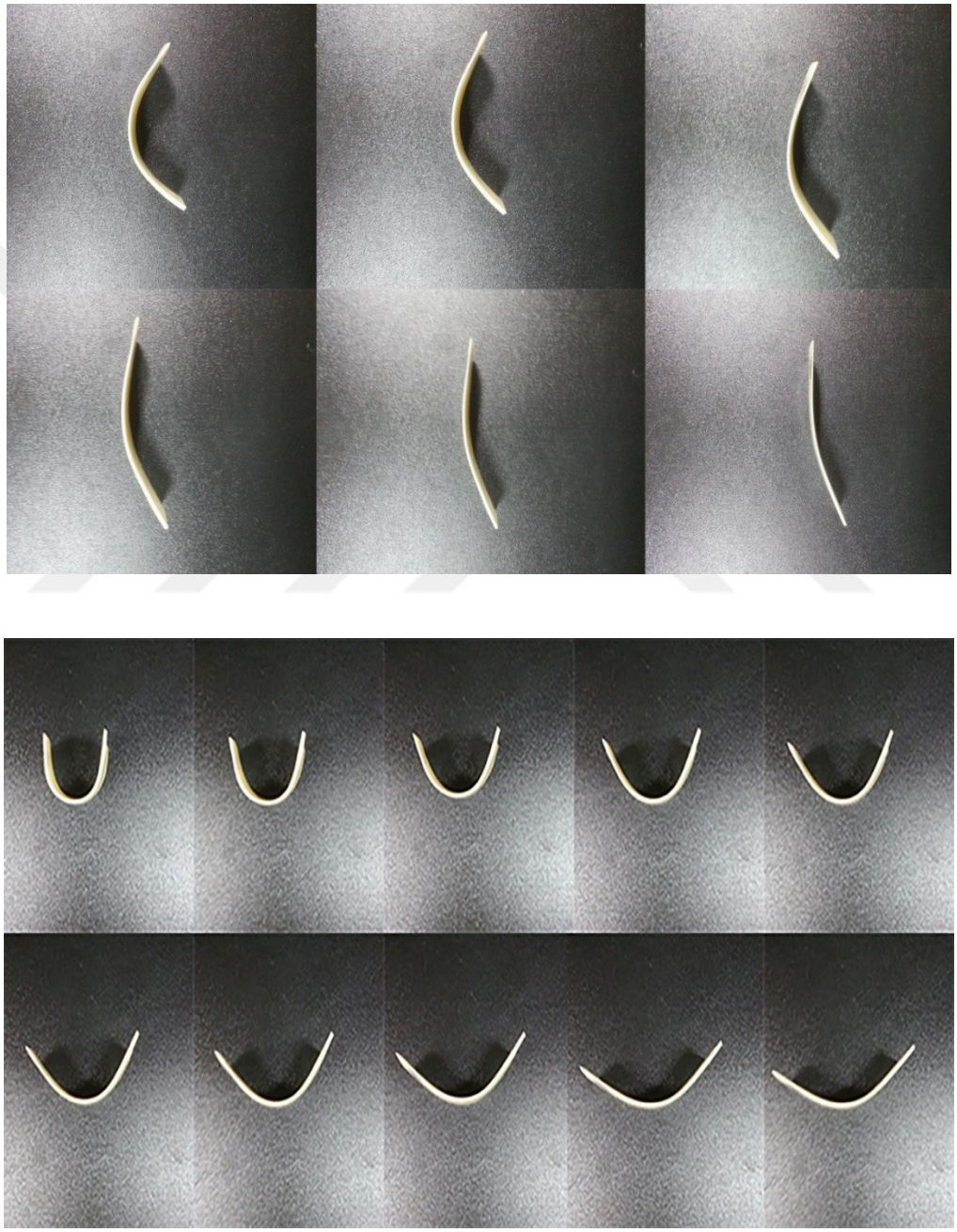

Figure 3.6: Shape memory effect in the PU specimens

3.2. METAL ALLOYS

3.2.1. Microstructure

Ti-Ni based specimens were produced by powder metallurgy method by using metal powders. Figure exhibits the SEM pictures of the (a) Ni, (b) Ti, (c) Co, (d) Sn powders.

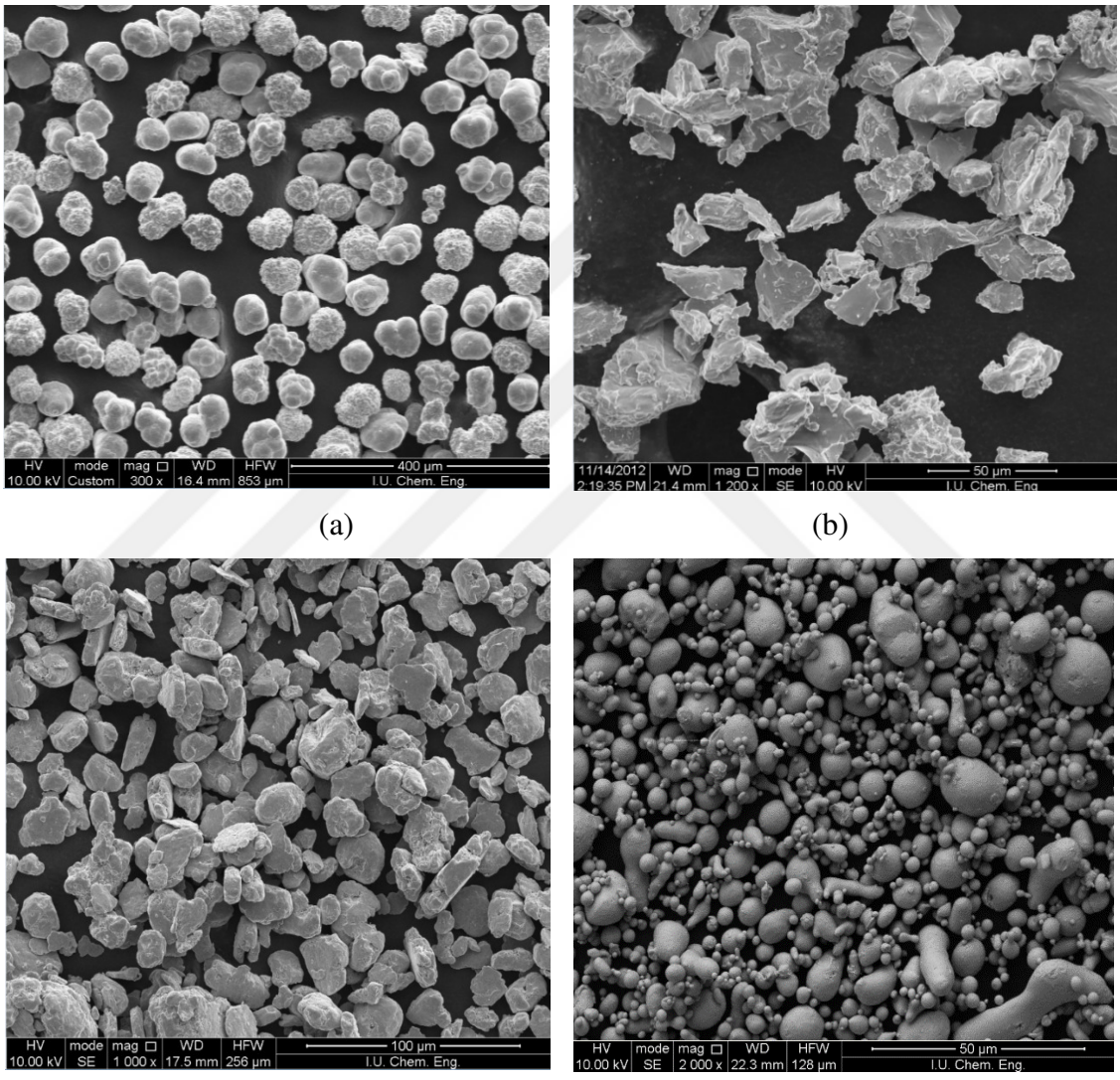

(a) (b)

(c) (d)

Figure 3.7: SEM picture of a) Ni, b) Ti, c) Co, d) Sn powders

Figure given below shows the SEM picture of the sintered Ti-Ni-Co-Sn alloy specimen. As seen from the Figure, there is a suitable sintering between the metal powder particles. There is no microcracks in the microstructure of the sintered alloy.

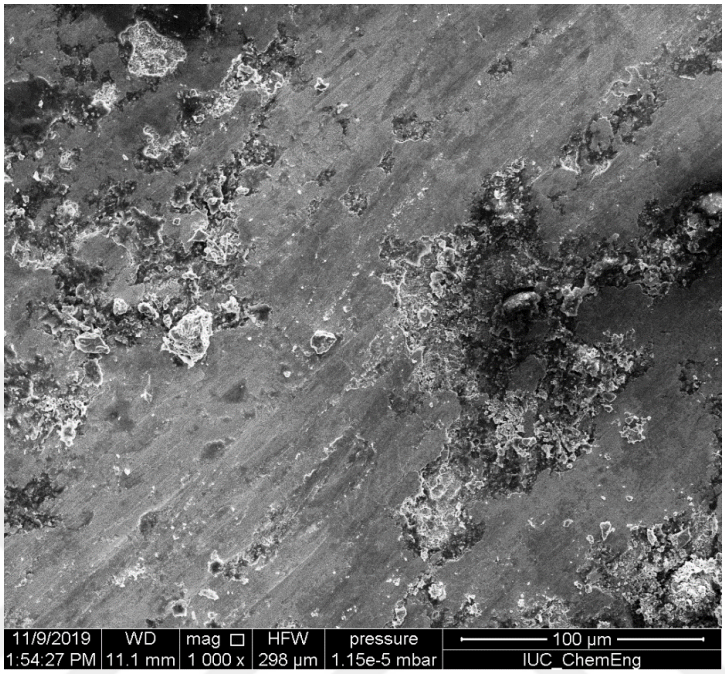

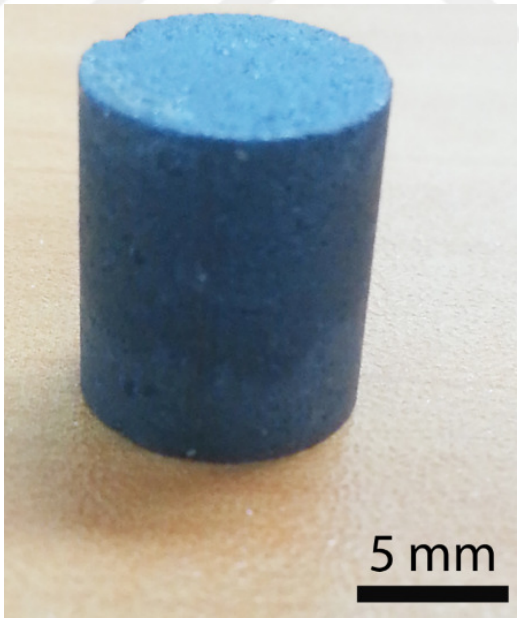

Figure 3.8: a) SEM picture of microstructure, b) photograph of sintered Ti-Ni alloy

XRD Results

Microstructure of the alloys was also characterized by x-ray diffraction (XRD) study. Figure given below shows the x-ray diffraction (XRD) patterns of the materials. Shape memory Ti-Ni alloys have partial solubility for the tin (Sn). Alloys show fine eutectic microstructures, which consisting of Ti_3Sn and Ti-Ni-Sn phases. Co did not formed intermetallic compound with titanium (Ti) and nickel (Ni).

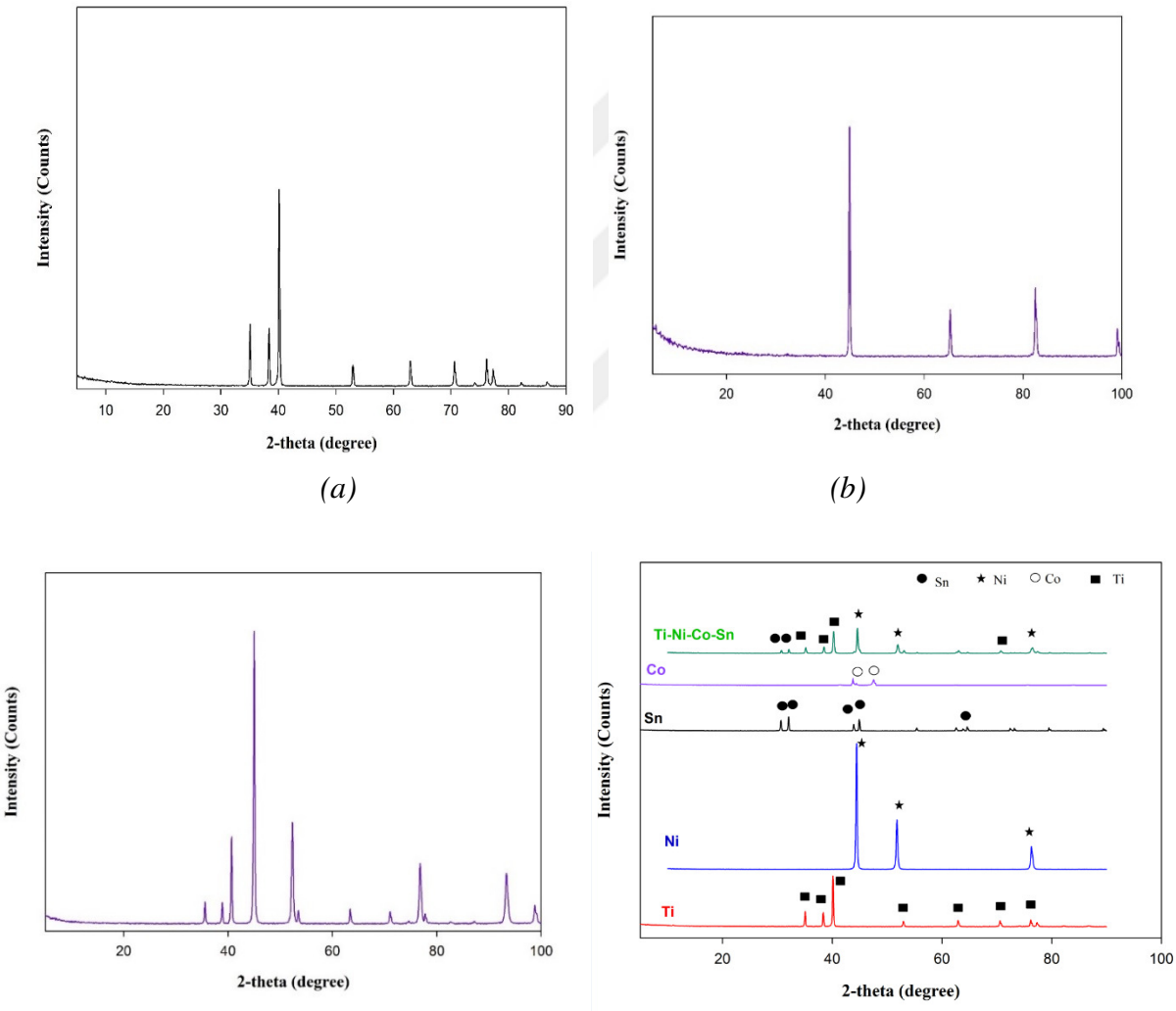

Figure 3.9: XRD results of the alloys a) Ti, b) Ni, c) Ti-Ni, d) Ti-Ni-Co-Sn alloys

Figure given below shows the (a) DSC graph of the Ti-Ni-Co-Sn alloy (b) DSC of the titanium-nickel (Ti-Ni) shape memory alloy, and (c) DTA of the titanium-nickel (Ti-Ni) alloy.

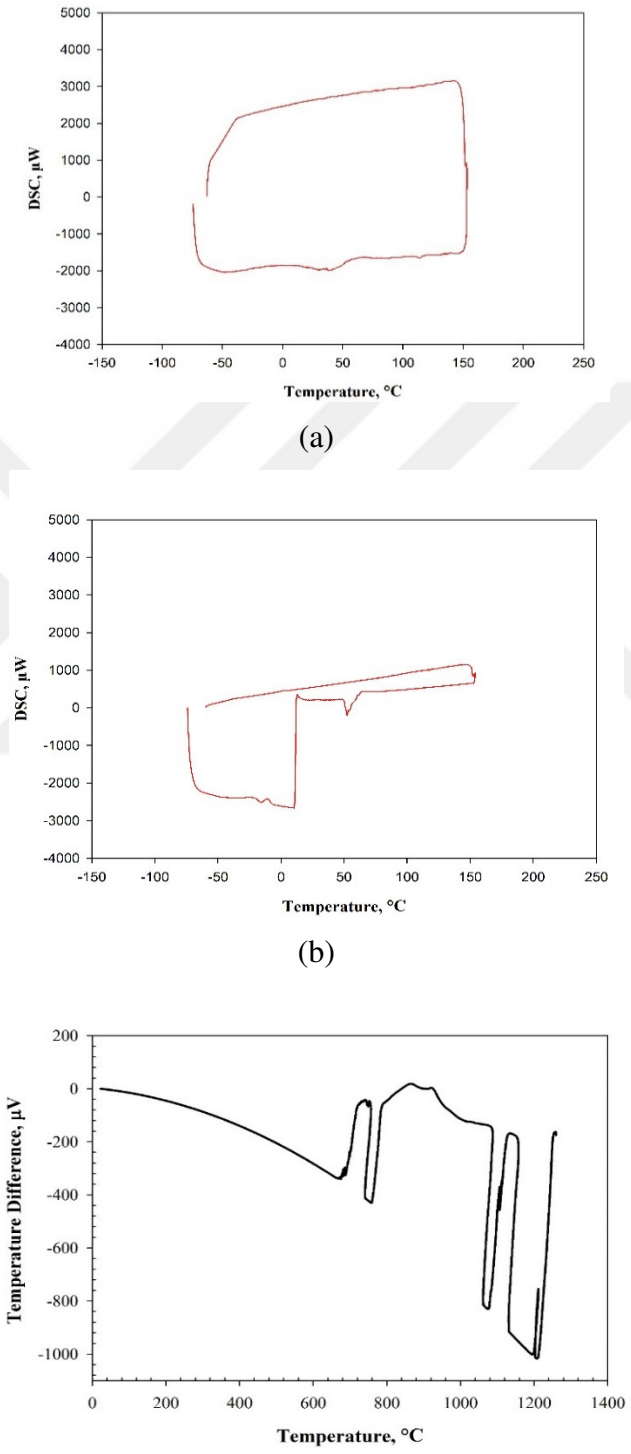

Figure 3.10: a) DSC of Ti-Ni-Co-Sn, b) DSC of Ti-Ni, c) DTA of Ti-Ni

Figure given below shows the effect of Co and Sn contents of the titanium-nickel (Ti-Ni) alloy on the Tafel polarisation curves. Tafel curves were employed to evaluate the electrochemical corrosion performance (corrosion potential and current density). In the Tafel curves, current density must be low, and corrosion potential must be high for low corrosion rate. As shown in the figure given below, increasing Co and Sn contents of the titanium-nickel specimens were lowered the corrosion potential and slightly increased the current density of the samples.

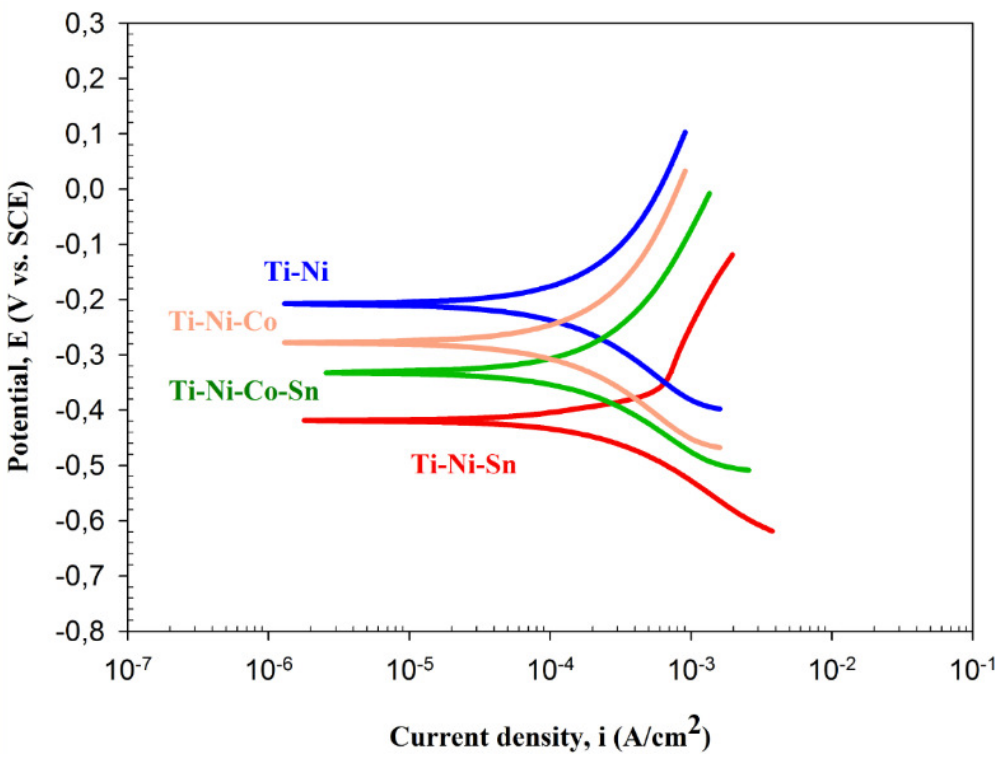

Figure 3.11: Corrosion test results of the alloys

Figure given below illustrates the effect of Co and Sn addition on the polarization resistance and corrosion rate of the titanium-nickel shape memory alloy. Polarization resistance of the specimens was decreased with the addition of Co and Sn additions. Corrosion rate of the titanium-nickel alloy samples was increased with the Co and Sn additions.

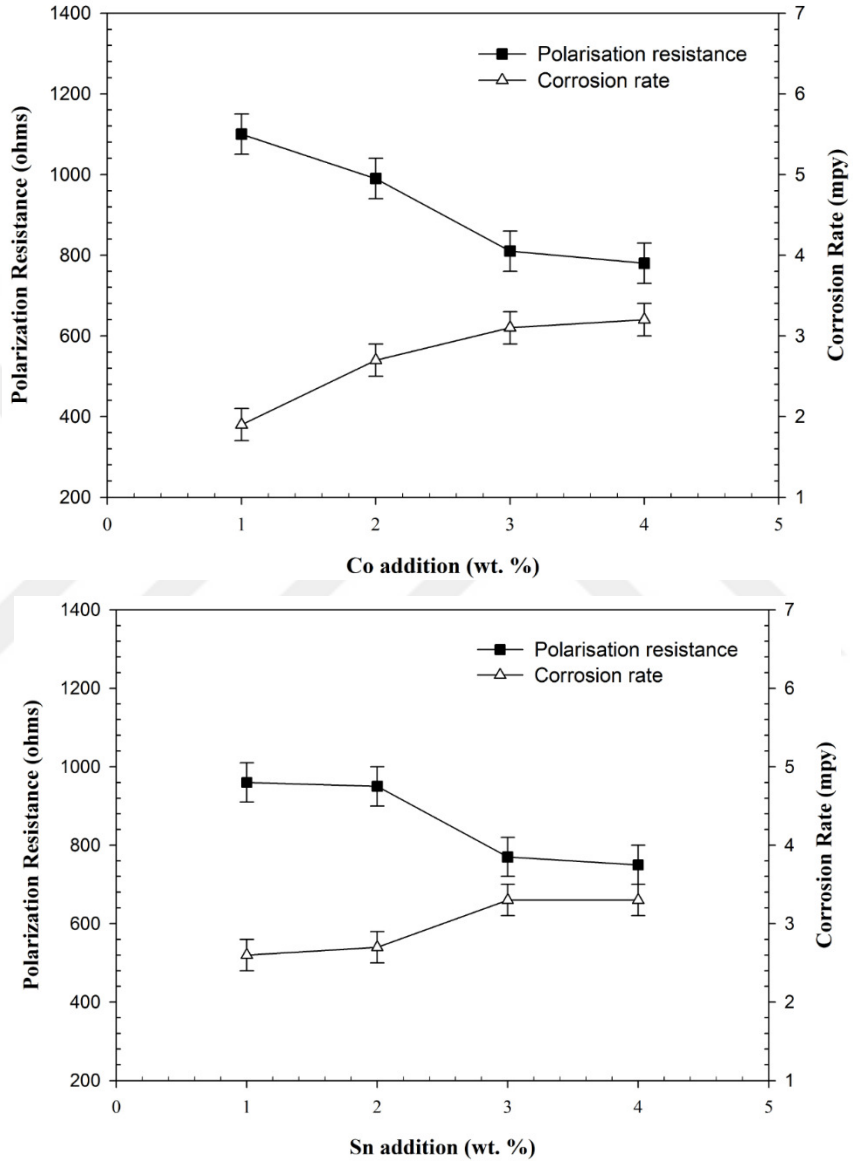

Figure 3.12: Effect of a) Co and b) Sn on polarization resistance and corrosion rate

3.2.2. Mechanical Properties

Figure given below exhibits the effect of sintering temperature on the (a) Young's modulus, and (b) yield strength of the samples. Young's modulus values of the specimens were increased with increasing sintering temperature. Increasing sintering temperature enhances densification of the material that results increases in the Young's modulus. In addition, compressive yield strength of the specimens was increased with increasing sintering temperature.

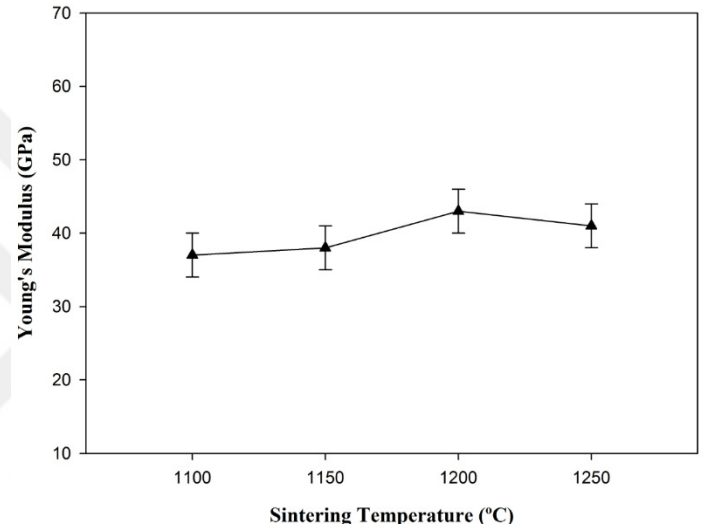

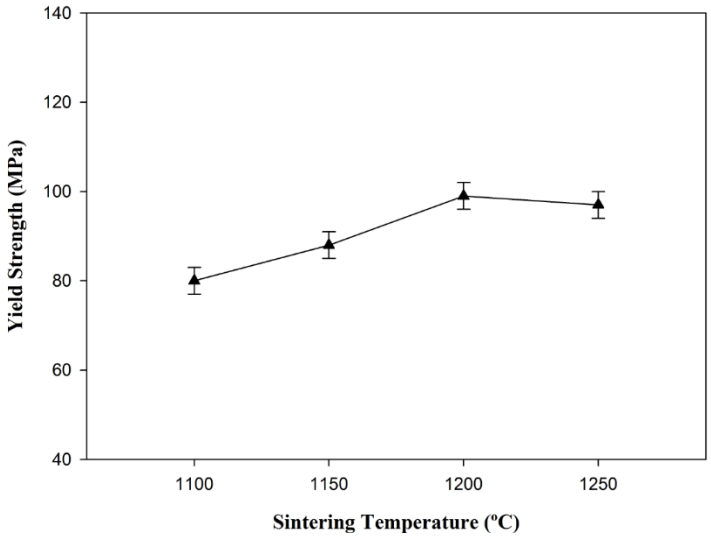

Figure 3.13: Effect of sintering temperature on a) Young's modulus, and b) yield strength

Figure given below shows the effect of aging temperature on the (a) Young's modulus, and (b) yield strength of the titanium-nickel based samples. Yield strength values of the Ti-Ni samples were increased with raising aging temperature and have shown superior properties at 400 °C. Initially, in the precipitation hardening, boundaries of Ti_3Ni_4 precipitates are coherent, and lattices distorted by the coherent stress field. As the precipitation hardening time raises, precipitates get bigger and lose their coherency.

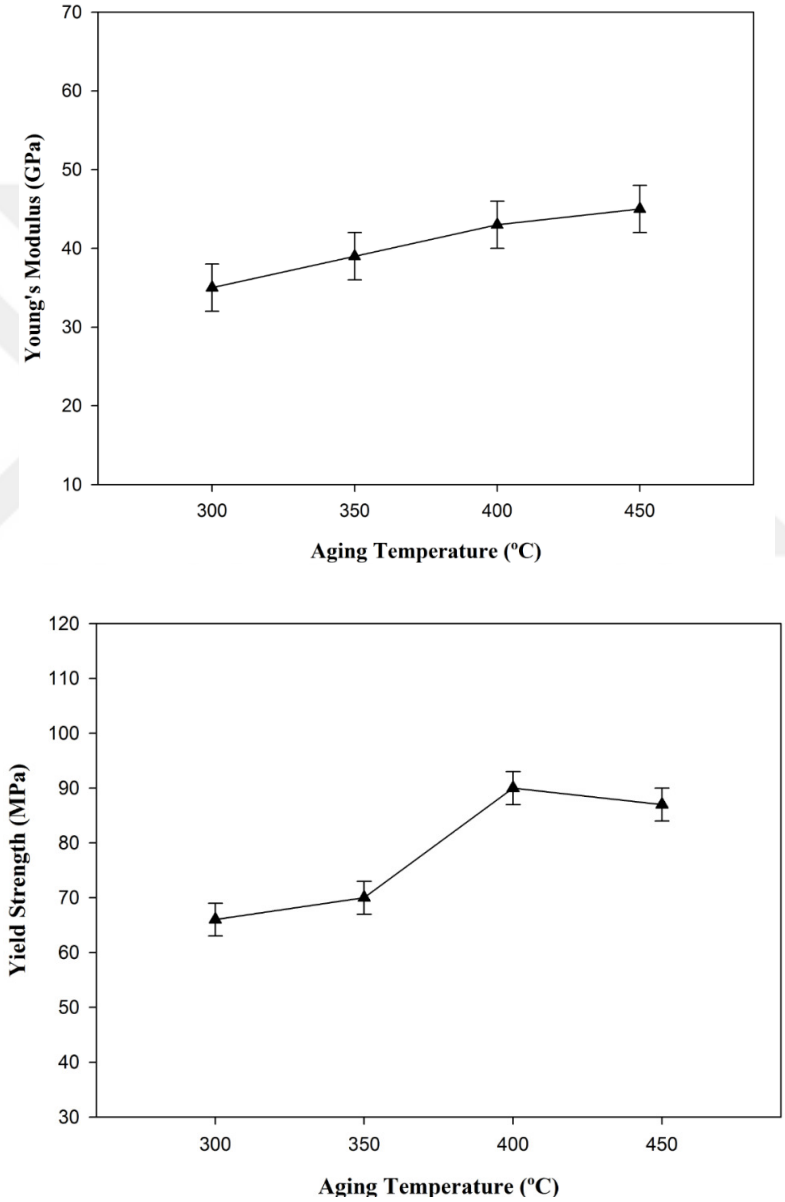

Figure 3.14: Effect of aging temperature on a) Young's modulus, and b) yield strength

Figure given below exhibits the effect of Co and Sn contents of the titanium-nickel alloys on the (a) Young's modulus, and (b) yield strength values. Increasing Co and Sn contents were increased the Young's modulus and compressive yield strength of the titanium-nickel based shape memory alloys. Co and Sn addition increased the mechanical properties by solid solution hardening. In addition, Sn addition was enhanced the sinterability of the alloy by liquid phase formation.

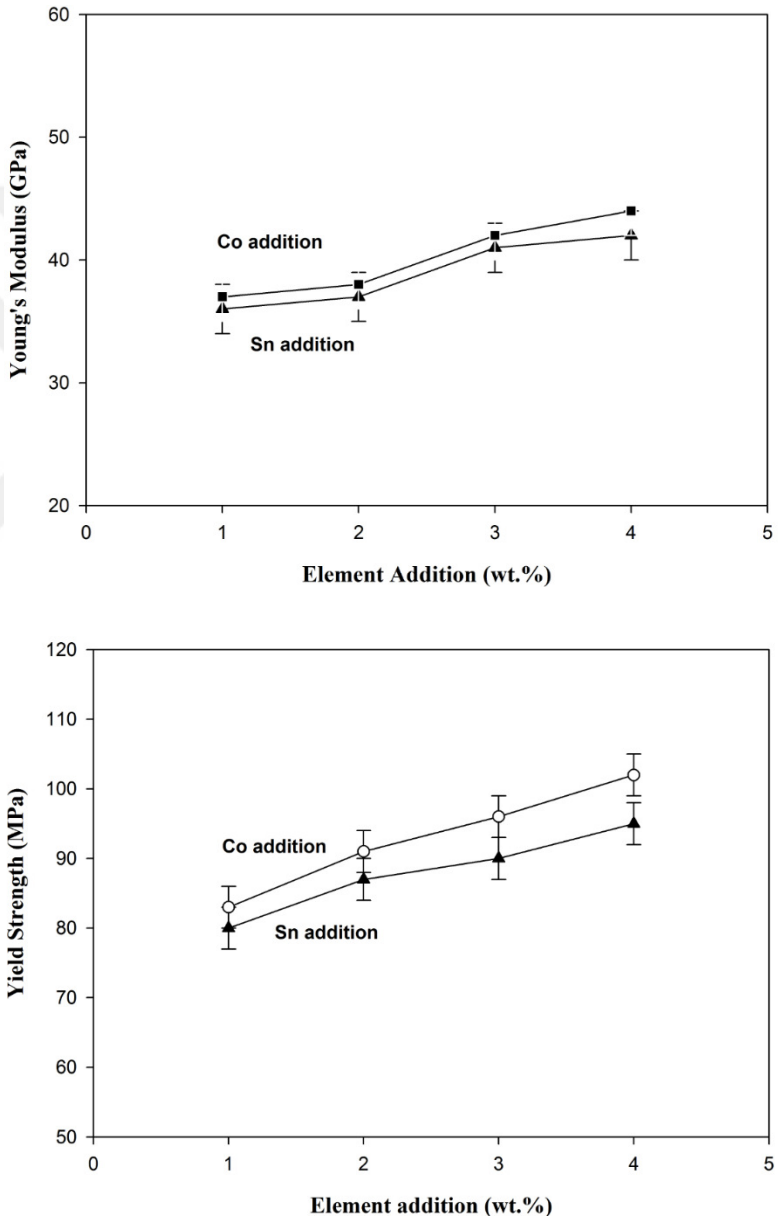

Figure 3.15: Effect of Co and Sn contents on (a) Young's modulus, and (b) yield strength

Figure shows the effect of temperature on the Young's modulus (martensite phase or austenite phase) of the titanium-nickel based shape memory alloys. Transformation temperature was 35-40 °C. As martensite and austenite phases have different elastic modulus values, martensite-austenite phase transformation temperature can be determined by ultrasonic velocity. Ultrasonic velocity is related to elastic modulus and density. Ultrasonic wave is influenced by microstructure. Elastic modulus of the titanium-nickel samples was determined by using a pulse-receiver type ultrasonic flaw detector.

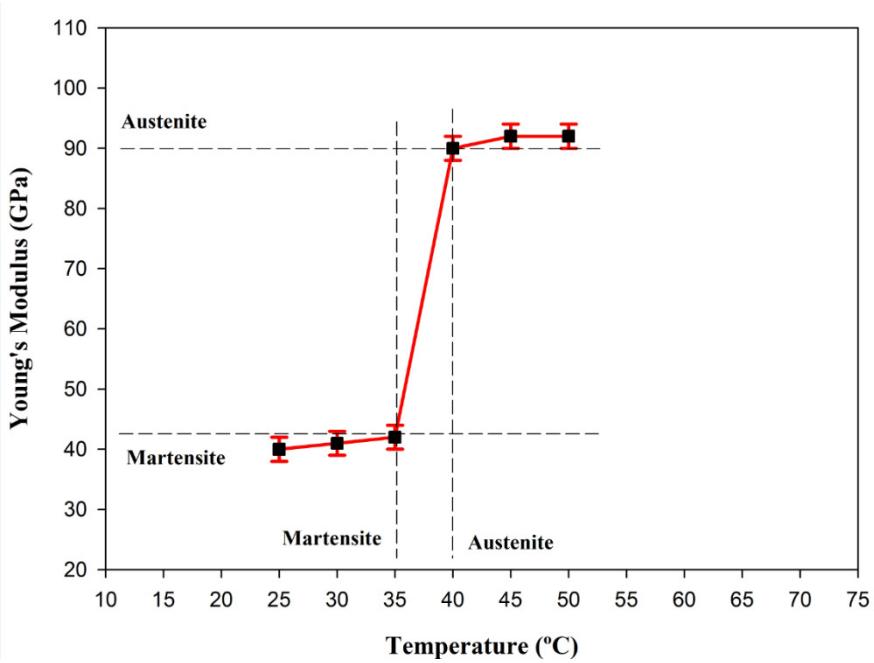

Figure 3.16: Effect of temperature on the Young's modulus (microstructure) of the alloy

4. DISCUSSION

In this thesis, manufacturing and characterization of mechanical type metamaterials (auxetic materials) and smart materials (shape memory titanium-nickel alloys) were carried out. Mechanical metamaterials were produced by additive manufacturing based rapid prototyping and replica method. In this process, firstly positive moulds (prototypes) were produced by stereolythografi based rapid prototyping method. Then, acrylic based photopolymer was used as a raw material. Then, silicone products (coronary stents, urethal sents, grafts) was produced by alginate molding (replica method) process. Several reinforcement materials was employed for the production of composite auxetic materials. In addition, auxetic polyurethane (PU) reinforced silicone matrix composites were also manufactured. Shape memory nickel-titanium (Ni-Ti) alloys were manufactured by the powder metallurgy (PM) and powder injection moulding (PIM) techniques.

Deformation mechanism of the auxetic (mechanical metamaterial) polyurethane (PU) specimen was found to be similar to the theoretical deformation of the auxetic meta-materials. Auxetic specimens were become denser with raising time. As the unit cell geometry is different with respect to applied external force, lateral and vertical compression behaviours of the auxetic samples were different. Deformation mechanism of TiO_2 reinforced auxetic polyurethane (PU) specimen was similar to theoretical deformation mode of the auxetic meta-materials. As the unit cell geometry is different with respect to the applied external force, lateral and vertical compression behaviours are different. Mechanical properties (strength, elastic modulus) of the composite polyurethane (PU) specimens were higher. Deformation mechanism of the auxetic (mechanical meta-material) specimen was similar to the theoretical deformation mode of the auxetic meta-materials.

In general, the shape memory titanium-nickel (Ti-Ni) based alloys have partial solid solubility for the tin (Sn). Titanium-nickel based shape memory alloys show very fine eutectic microstructures, which consisting of Ti_3Sn and Ti-Ni-Sn phases. Co addition did not formed intermetallic compound with the titanium (Ti) and nickel (Ni).

Tafel curves were employed to evaluate the electrochemical corrosion performance (corrosion potential and corrosion current density). Increasing Co and Sn contents of the titanium-nickel

based alloys were lowered the corrosion potential and slightly increased the current density of the samplesi as expected. Polarization resistance of the titanium-nickel based specimens was decreased with the addition of Co and Sn elements. The corrosion rate of the titanium-nickel based samples was increased with the Co and Sn element additions.

Young's modulus values of the titanium-nickel based specimens were increased with raising sintering temperature. Increasing sintering temperature enhances the densification of the material that results increases in the Young's modulus of the titanium-nickel based alloys. In addition, compressive yield strength of the titanium-nickel based specimens was increased with raising sintering temperature. Yield strength values were increased with increasing aging temperature and have shown suitable properties at about 400 °C.

Transformation temperature of the titanium-nickel based shape memory alloys was about 35-40 °C. As the martensite and austenite phases have different elastic modulus values from each other, the martensite-austenite phase transformation temperature can be determined by using ultrasonic velocity.

In general, the shape memory effect (SME) in the titanium-nickel based alloys is dependent on the composition and thermal treatments. Variation of Ni content shifts the transformation temperatures.

Precipitations, causes migration of Ni atoms to participates, which leads to increase in transformation temperatures. At high temperatures, precipitates 400 °C was found to be the best aging temperature (balance between driving force and diffusion). Small amount Co and Sn additions to the Ti-Ni based alloys decrease the transformation temperature.

5. CONCLUSION AND RECOMMENDATIONS

In this thesis, manufacturing and characterization of mechanical type metamaterials (auxetic materials) and smart materials (shape memory titanium-nickel alloys) were carried out. Mechanical metamaterials were produced by additive manufacturing based rapid prototyping and replica method. In this process, firstly positive moulds (prototypes) were produced by stereolythografi based rapid prototyping method. Then, acrylic based photopolymer was used as a raw material. Then, silicone products (coronary stents, urethal sents, grafts) was produced by alginate molding (replica method) process. Several reinforcement materials was employed for the production of composite auxetic materials. In addition, auxetic polyurethane (PU) reinforced silicone matrix composites were also manufactured. Shape memory nickel-titanium (Ni-Ti) alloys were manufactured by the powder metallurgy (PM) and powder injection moulding (PIM) techniques.

In this study, Ti-Ni based shape memory specimens were produced by powder metallurgy technique. Effects of process parameters on the mechanical properties were investigated. Elastic modulus of the specimens was characterized by destructive compression tests and non-destructive ultrasonic tests. Nondestructive ultrasonic test was employed to investigate the elastic modulus and microstructure (martensite and austenite phases). Martensite-austenite phase transformation temperature was investigated by using ultrasonic velocity measurements. Microstructure and electrochemical corrosion properties of the titanium-nickel alloys were also investigated. Traditional casting based production and forming process is not suitable to obtain a homogeneous material. Chemical compositions of titanium-nickel (Ti-Ni) shape memory alloys because of the segregation due to the density differences of the alloying elements. Segregation in the solid-state powder metallurgy based alloys is relatively small.

Effects of the process parameters (sintering temperature, aging temperature) on the mechanical properties of the Ti-Ni samples were investigated. Microstructure and electrochemical corrosion properties of the titanium-nickel samples were also investigated. Young's modulus and strength values of the titanium-nickel specimens were enhanced with raising sintering temperature. Increasing sintering temperature enhances densification of the material that results increases in the mechanical properties.

Raising Co and Sn content of the Ti-Ni alloy was lowered the corrosion potential and increased the corrosion current density. Moreover, corrosion properties of the titanium-nickel samples were changed with the aging process. According to the electrochemical corrosion tests, aged titanium-nickel specimens were corroded more severely than non-aged ones.

REFERENCES

[1] Şengör, İ., 2013, Shape memory polymer composites containing carbon based fillers, Yüksek Lisans Tezi, Ortadoğu Teknik Üniversitesi, Fen Bilimleri Enstitüsü, Kimya Mühendisliği.

[2] Yu X., Zhou J., Liang H., Jiang Z., Wu L., 2018, Progress in Materials Science 94, 114-173.

[3] Ren X., Das R., Tran P., Ngo T.G., Xie Y.M., 2018, Smart Mater. Struct. 27, 114-173.

[4] Jani J.M., Leary M., Subic A., Gibson M.A., 2014, Materials and Design. 56, 1078-113.

[5] Ma J., Karaman I., Noebe R.D., 2010, Materials and Design. 55, 257-315.

[6] Leng J., Lan X., Liu Y., Du S., 2011, Materials and Design. 56, 1077-1135.

[7] Yang Y., Urban M.W.., 2013, Chem Soc. Rev. 42, 7446.

[8] Ak, E., 2010, Stress and Deformation Analysis in Stents, Yüksek Lisans Tezi, Marmara Üniversitesi, Fen Bilimleri Enstitüsü, Makine Mühendisliği.

[9] O'Brien B., Zafar H., Ibrahim A., Zafar J., Sharif F., 2016, Annals of Biomedical Engineering. 44, 2, 523-535.

[10] Park J.B., Bronzino J.D.. 2007, Biomaterials, Principles and Applications, CRC Press, New York, USA.

[11] Ratner, B. 2004, Biomaterials Science, An Introduction to Materials in Medicine, Elsevier.

[12] Shashi G.M., Laskar A.R.,Biswas H.,Saha A.K., 2017, Proceedings of 14th Global Engineering and Technology Conference.

[13] Wong K.V., Hernandez A., 2012, International Scholarly Research Network, 1-10.

[14]. Upadhyaya, G.S., 2002. *Powder Metallurgy Technology*, Cambridge International Science Publishing, England.

[15]. Engin, G., 2013, *Mikro Gözenekli Titanyum Parçaların Toz Enjeksiyon Kalıplama Yöntemiyle Üretilmesi Ve Karakterizasyonu*. Marmara Üniversitesi, Fen Bilimleri Enstitüsü, Yüksek Lisans Tezi.

[16]. ASM Handbook, 1998, *Powder Metal Tehnologies and Applications, Volume 7,* ASM International.

[17] Yuan S., Chua C.K., Zhou K., 2019, Adv. Mater. Tech., 4, 1800419.

[18] Wang H., Zhang Y., Lin W., Qin Q.H., 2020, Computational Materials Science, 171, 109232.

[19] Jabur A.S.., Al-Haidary J.T.., Al-Hasani E.S., 2013, Journal of Alloys and Compounds, 578, 136-142.

[20] Eda T., Khantachawana A., Umeda J., Kondoh K., 2019, Materials Transactions, 60, 8, 1583-1590.

[21] Liu B., Zheng Y.F., Ruan L., 2011, Materials Transactions, 65, 540-543.

CURRICULUM VITAE

Personal Information	
Name Surname	Mohamad ATTAR
Place of Birth	Aleppo/Suriye
Date of Birth	14.01 1989
Nationality	❒ T.C. ☑ Other: 99626255420
Phone Number	0534 327 65 99
Email	muhammad.attar1212@gmail.com
Web Page	



Educational Information	
B. Sc.	
University	
Faculty	
Department	
Graduation Year	Tarih girmek için tıklayın veya dokunun.

M. Sc.	
University	Istanbul University-Cerrahpasa
Institute	Institute of Graduate Studies
Department	Nanoscience and Nanoengineering
Programme	Nanoscience and Nanoengineering

Ph. D.	
University	
Institute	
Department	
Programme	

Publications